June 2 – 6, 2025
at Principia Institute, São Paulo, Brazil

June 6, 2025

KISS project – Spectroscopy of neutron-rich nuclei near *N* = 126 and actinides toward elucidating r-process nucleosynthesis

WNSC, IPNS, KEK
Yutaka Watanabe

Contents

1. Physics motivation
2. Nuclear production by MNT reactions
3. KISS facility
4. Experimental results around *N* = 126 and actinides
5. Beyond KISS
6. Summary

KEK Wako Nuclear Science Center

Nucleosynthesis in the universe

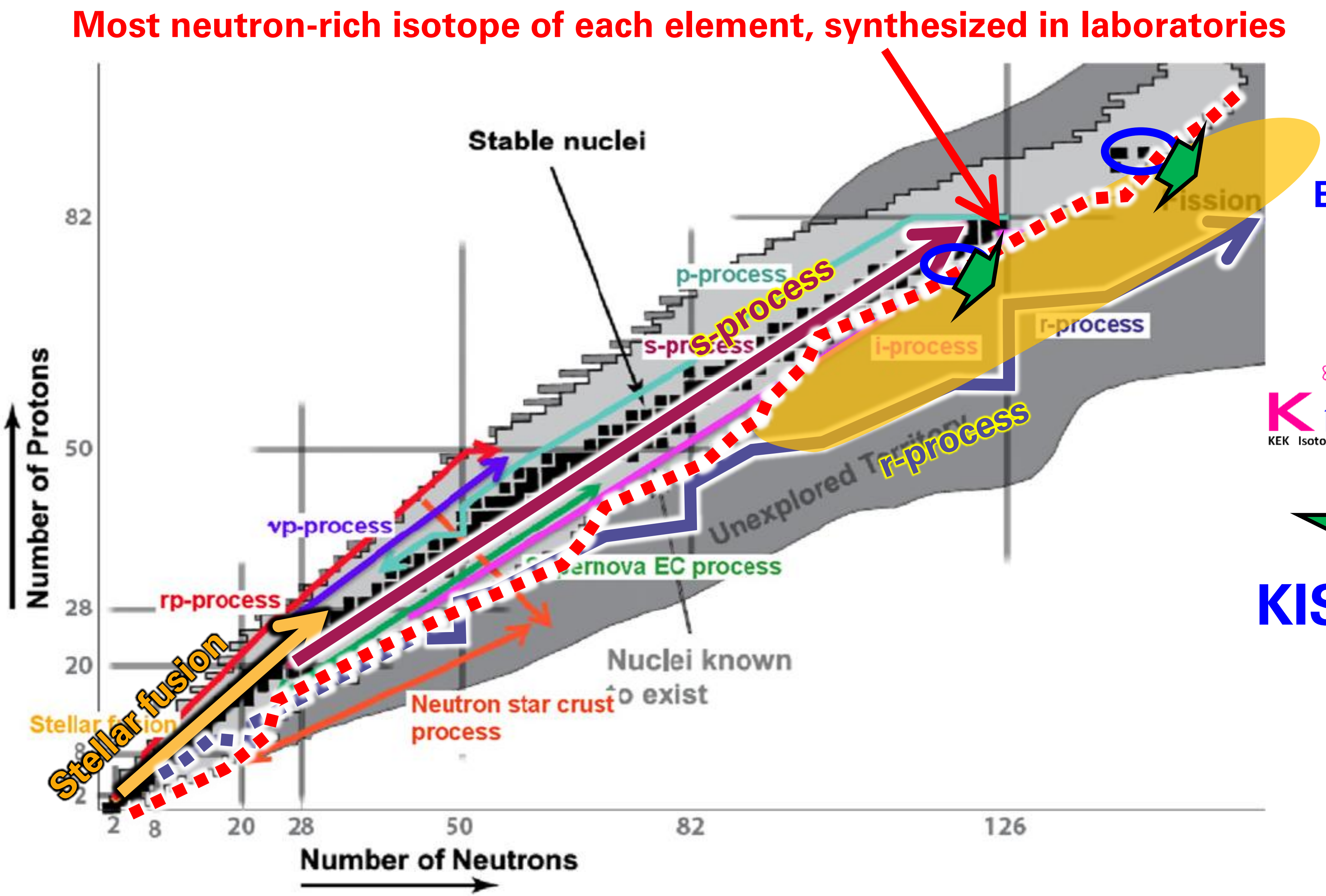

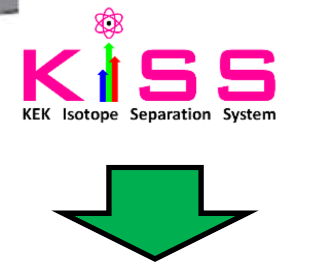

H. Schatz, J. Phys. G: Nucl. Part. Phys. 43, 064001 (2016).

Spectroscopy of neutron-rich nuclei around *N* =126

r-process nucleosynthesis

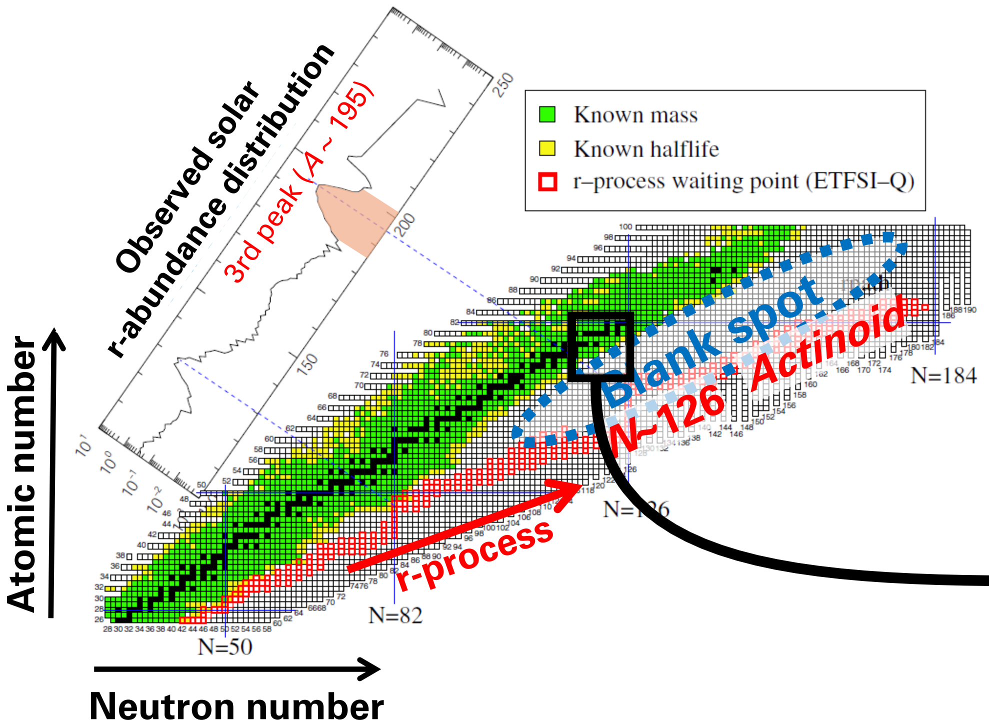

H. Grawe et al., Rept. Prog. Phys. 70, 1525 – 1582 (2007).

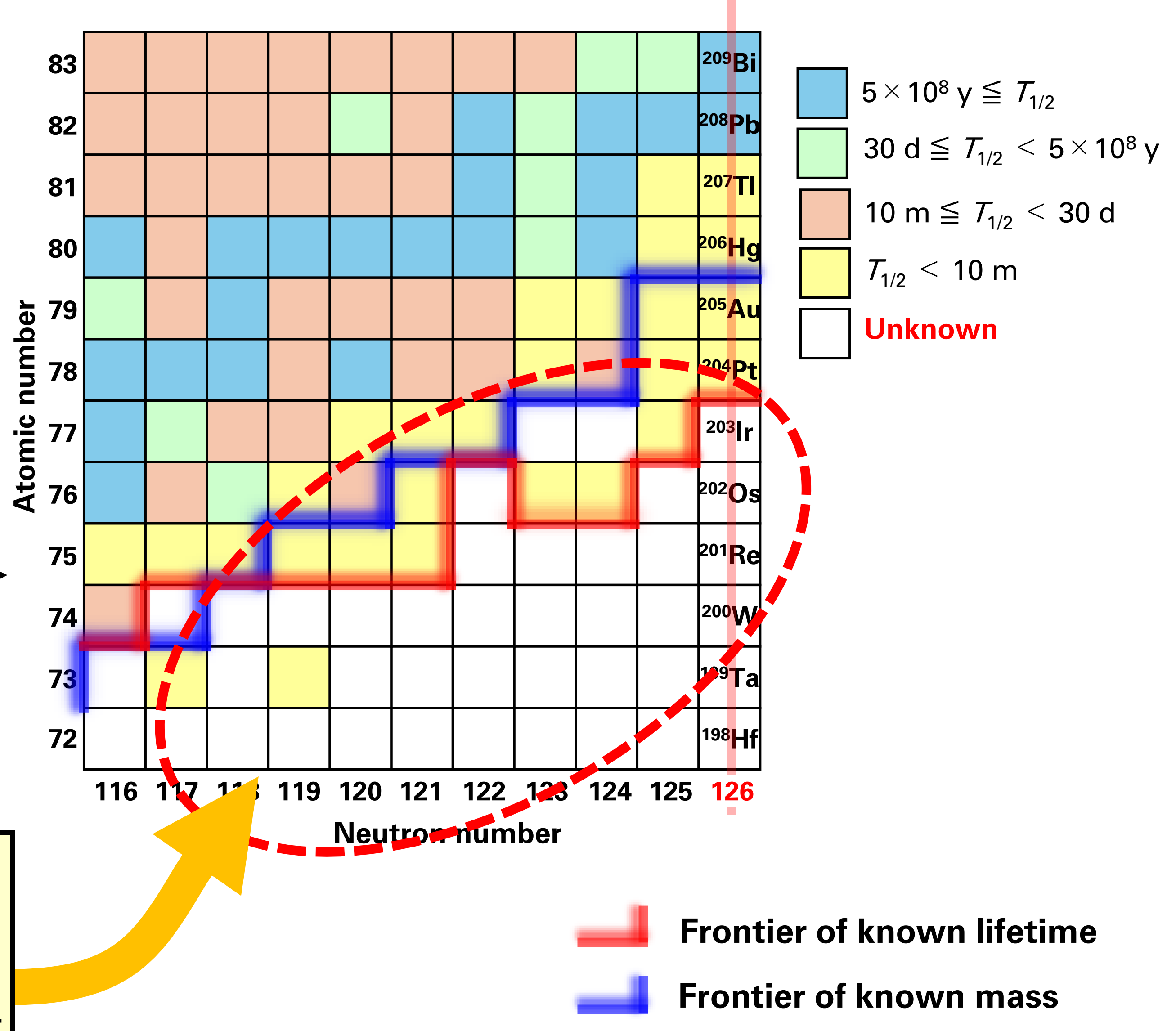

- ◆ **Decay spectroscopy**
  - ➢ **Half life**
  - ➢ **Decay scheme**
- ◆ **Laser spectroscopy**
  - ➢ **Charge radius**
  - ➢ **Magnetic dipole moment**
  - ➢ **Electric quadrupole moment**
- ◆ **Mass spectrometry**

Uncertainty of lifetime and r-abundance

Deviation of r-abundance pattern by uncertainty of β-decay half-life $(0.1 \sim 10 \times T_{1/2})$

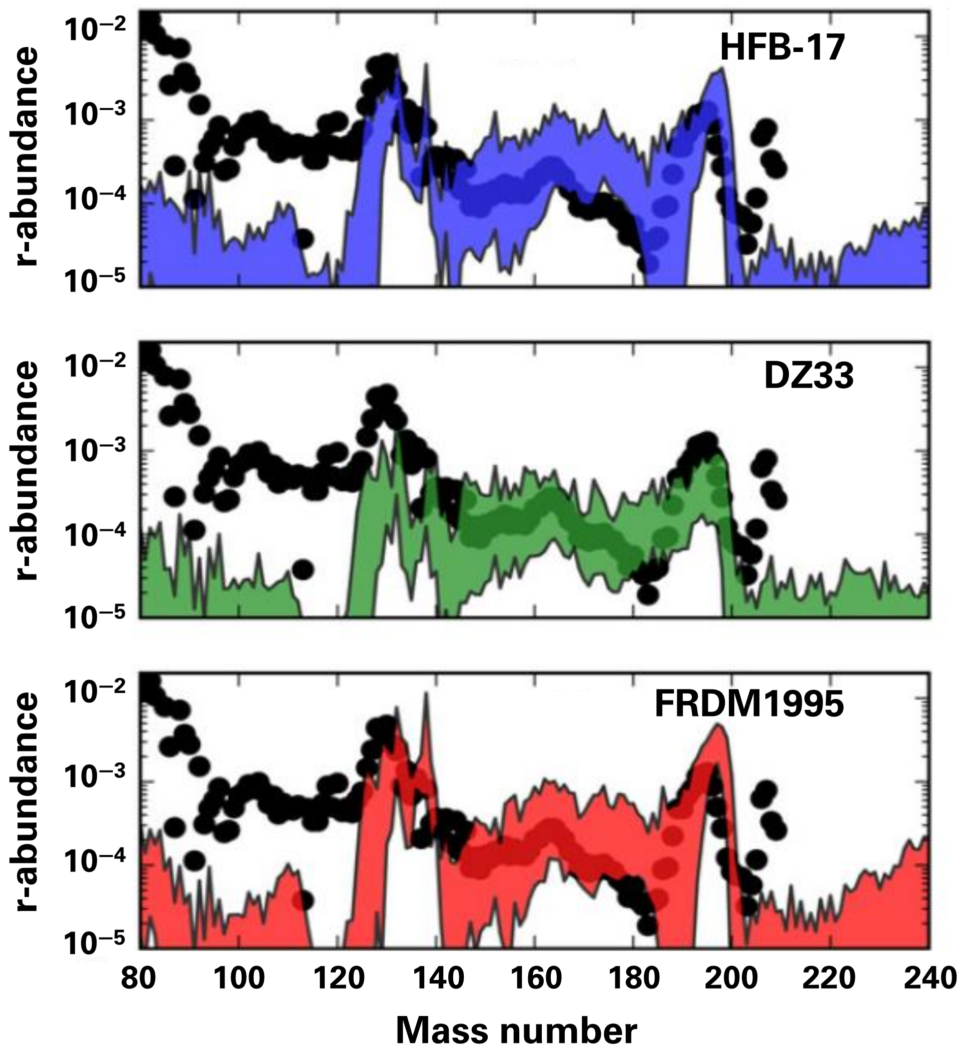

Sensitivity of r-abundance pattern to lifetime uncertainty $(0.1 \sim 10 \times T_{1/2})$

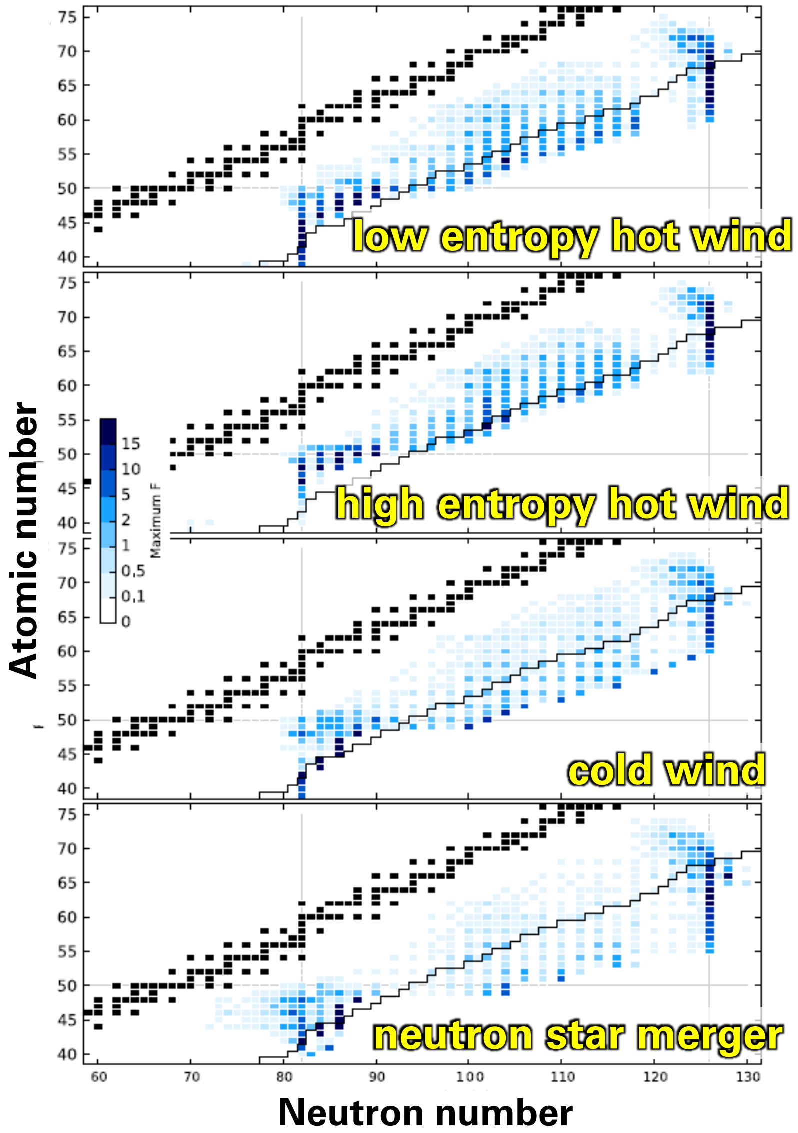

M.R. Mumpower et al., Prog. Part. Nucl. Phys. 86, 86 (2016).

Theoretical prediction of half-lives of $N = 126$ nuclei

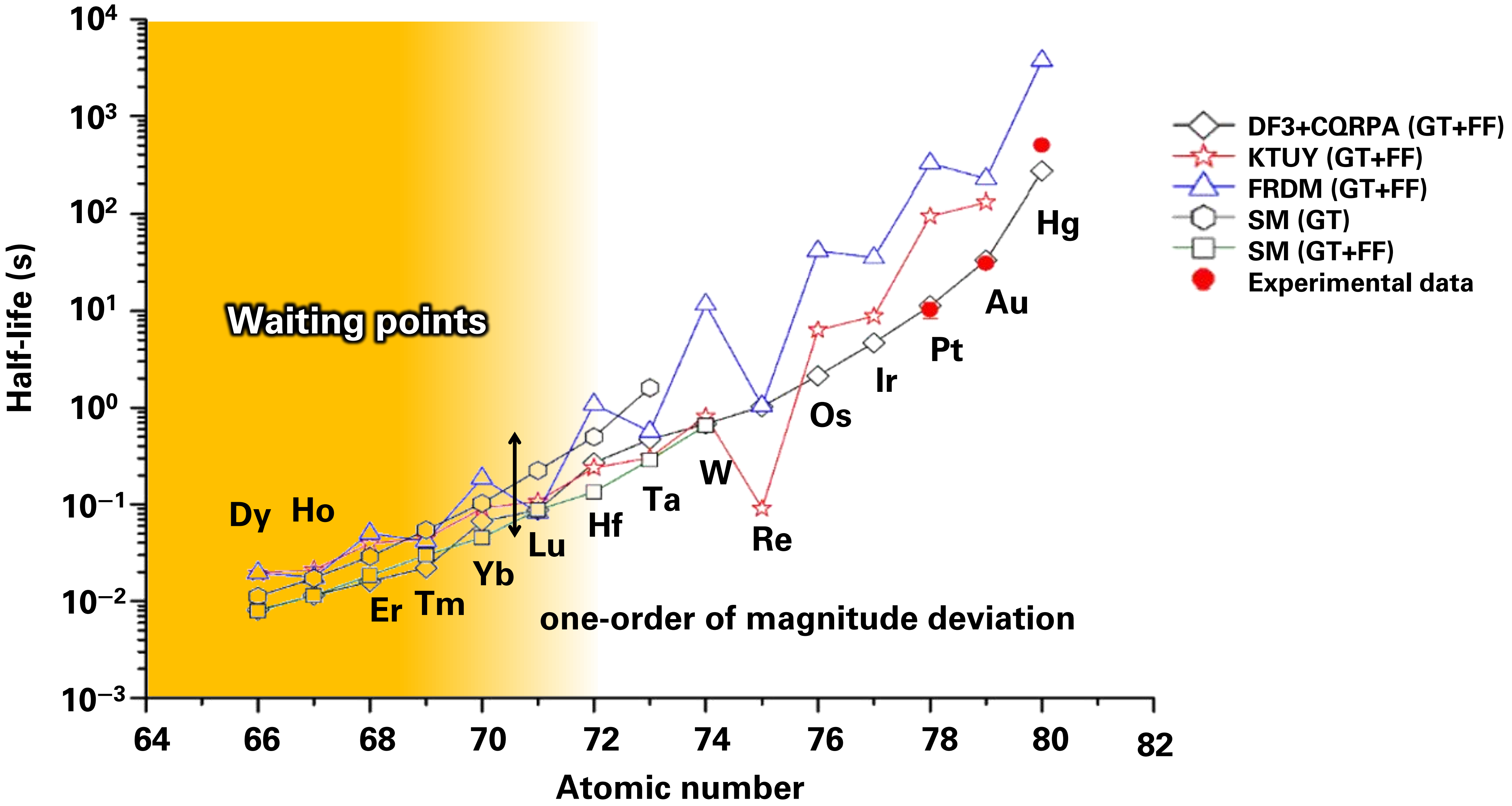

Competition between first-forbidden and allowed transitions

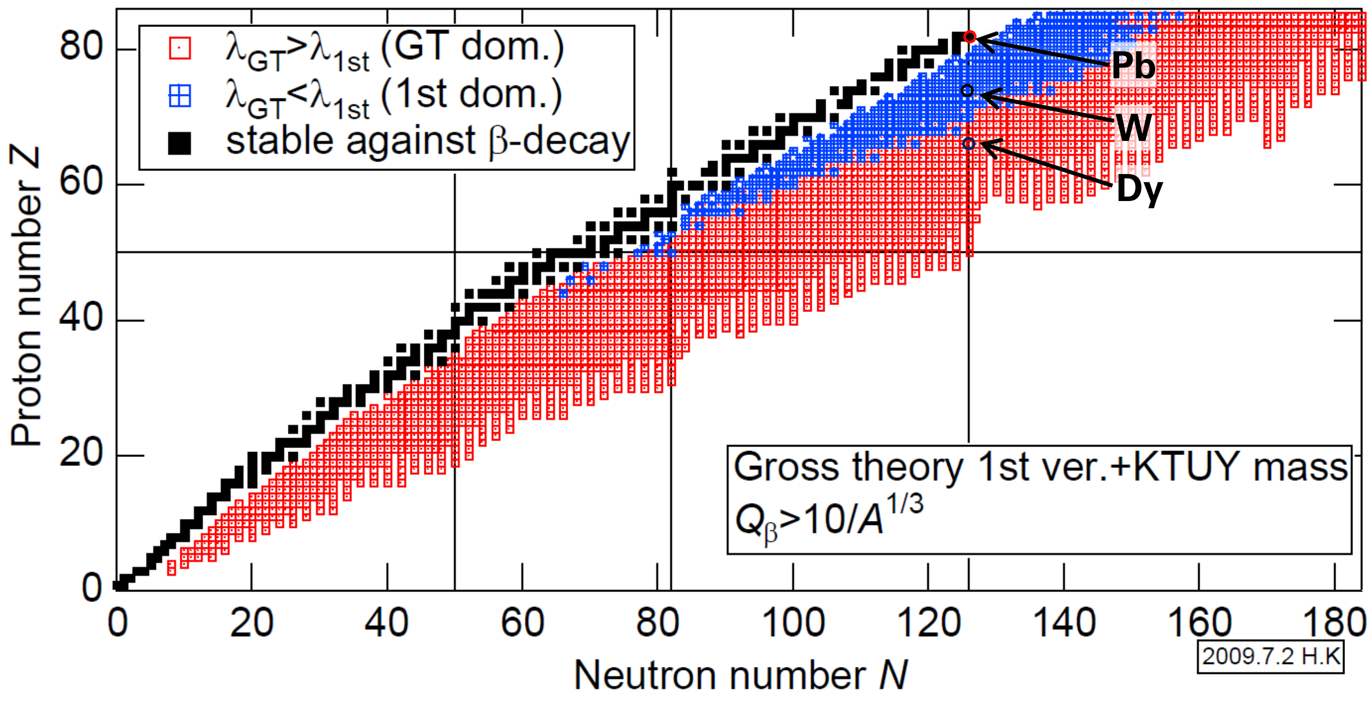

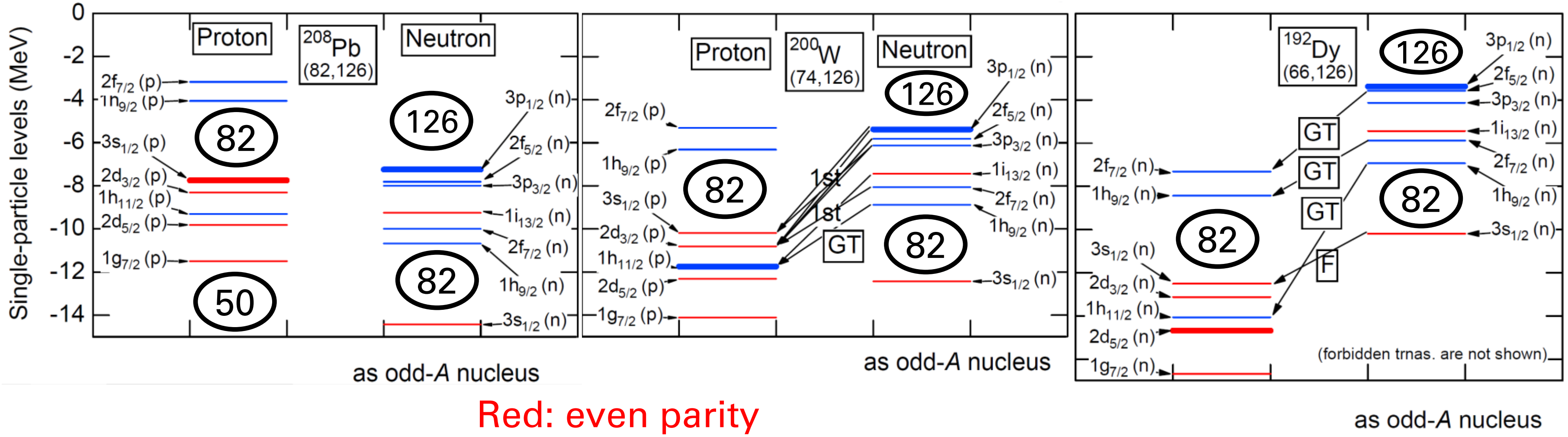

Red: even parity
Blue: odd parity

H. Koura, JAEA-Review 2010-056, pp.83–84 (2010).

Nuclear deformation

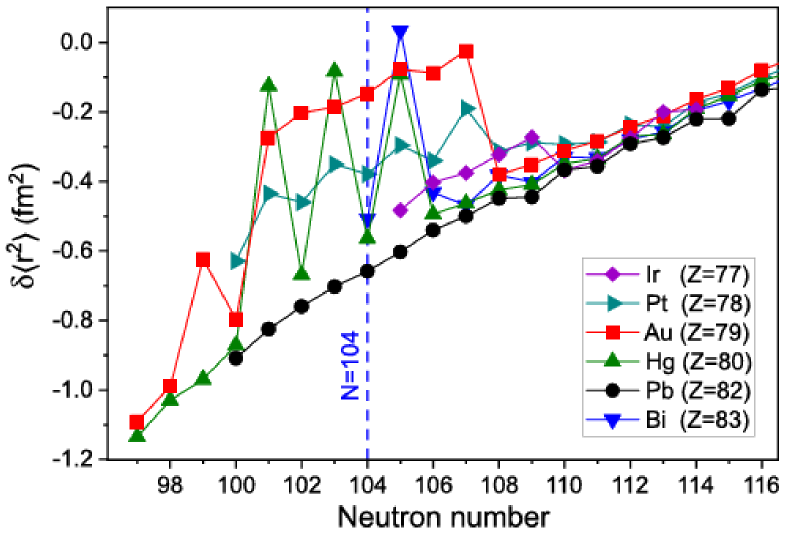

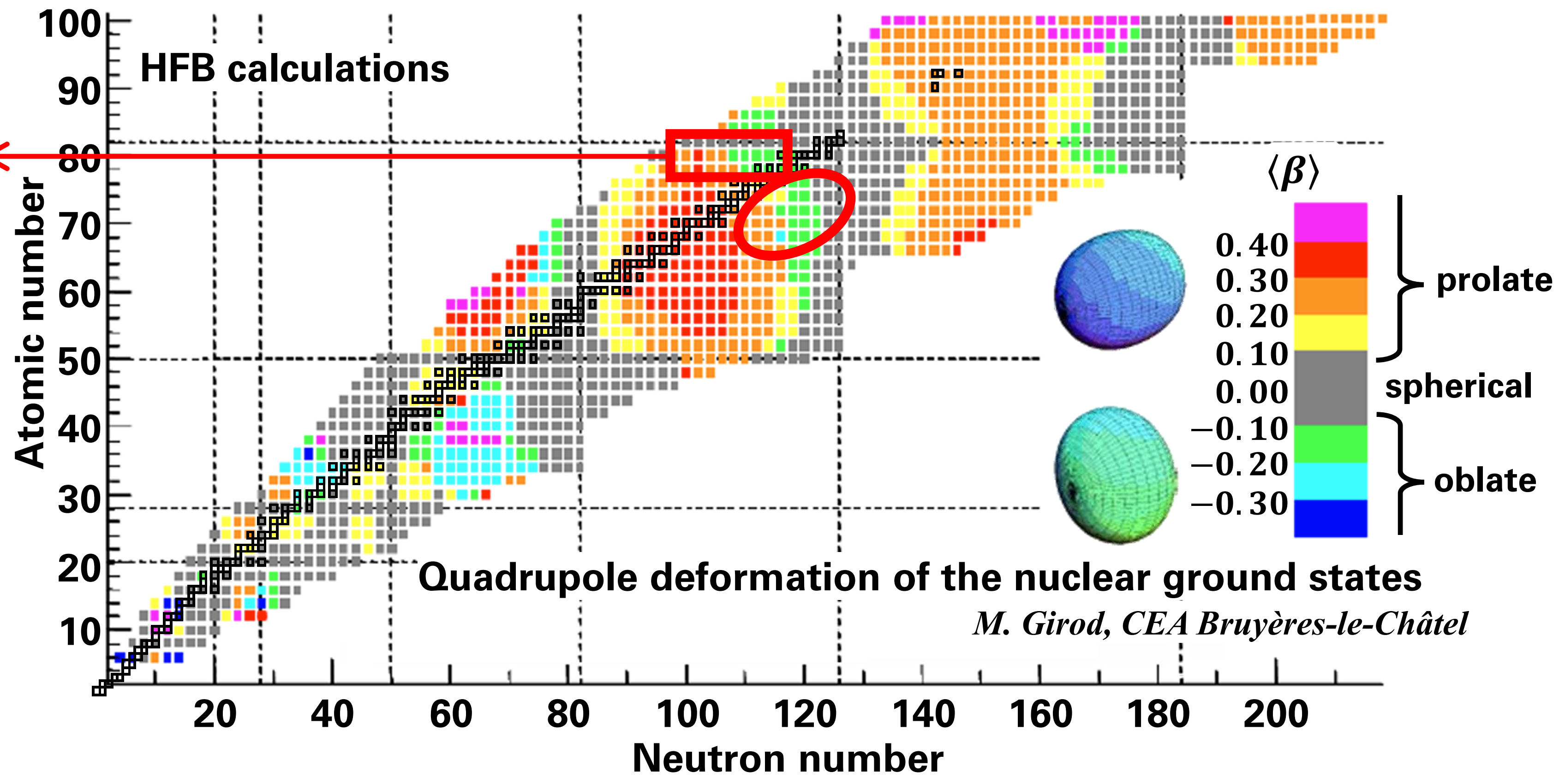

- The shape is one of the most fundamental properties of an atomic nucleus.
  Interplay of macroscopic properties of the nuclear matter and microscopic shell effects
- In some areas of the nuclear chart, the shape is very sensitive to structural effects and can change from one nucleus to its neighbor.
- Excitation energy, Angular momentum
  →Rearrangement of the orbital configuration, Dynamic response to nuclear rotation
  →Shape change
- Mixing of wave functions → Shape coexistence

Spectroscopy of neutron-rich nuclei around *N* =126

r-process nucleosynthesis

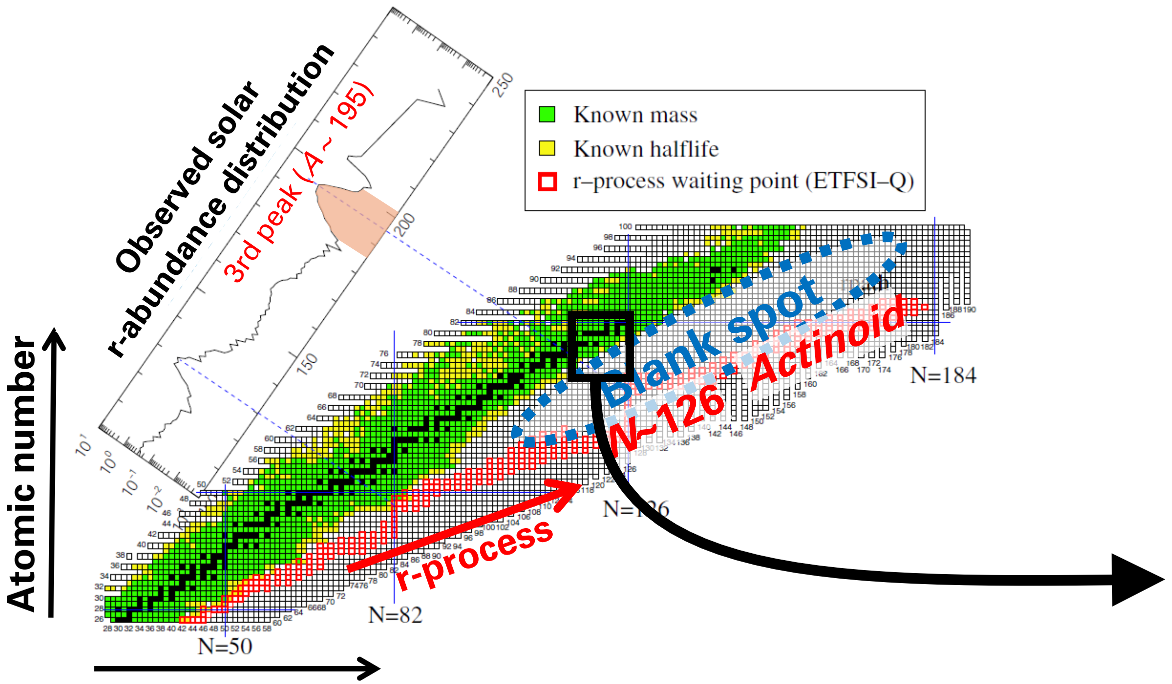

H. Grawe et al., Rept. Prog. Phys. 70, 1525 – 1582 (2007).

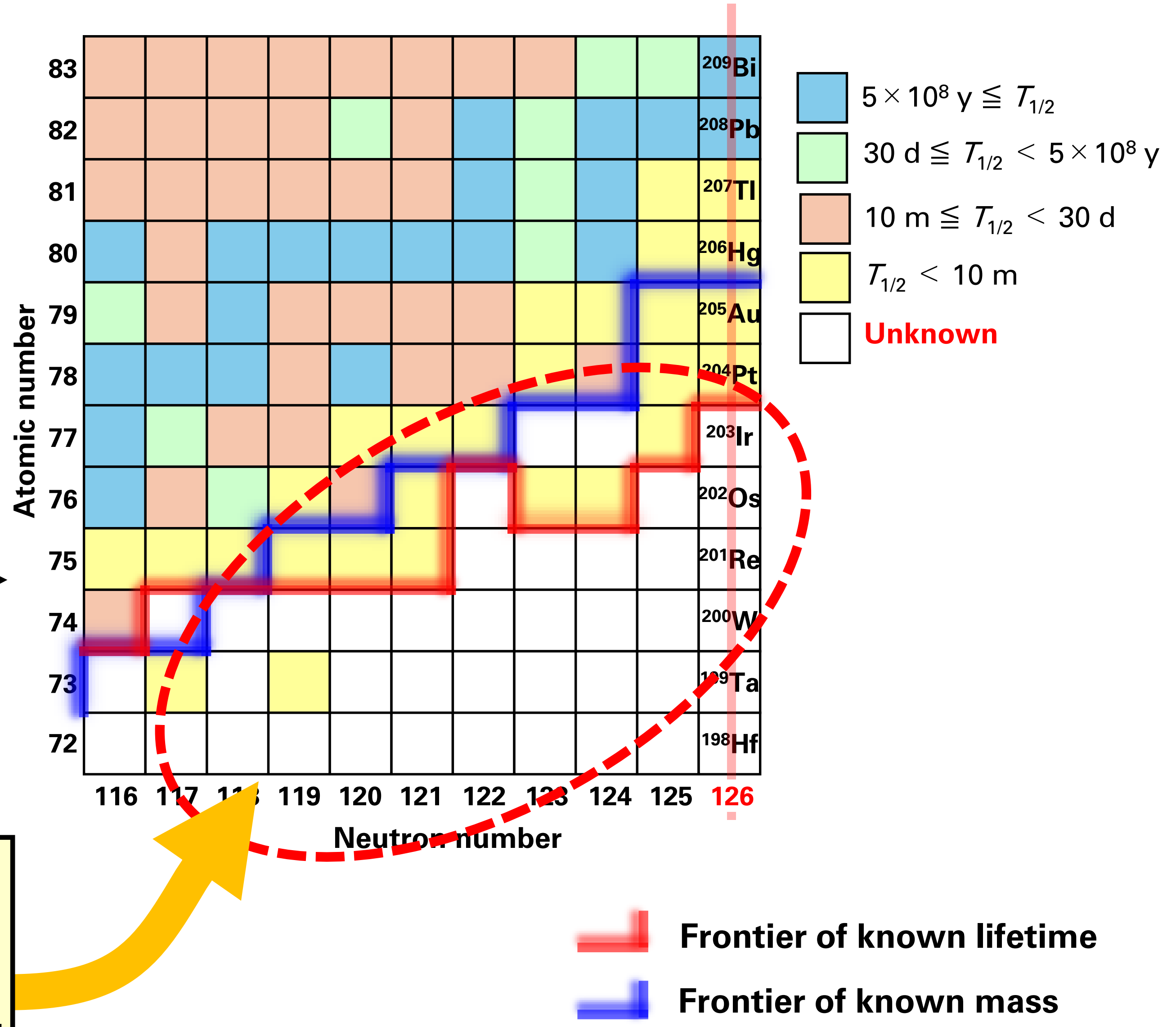

- **Decay spectroscopy**
  - **Half life**
  - **Decay scheme**
- **Laser spectroscopy**
  - **Charge radius**
  - **Magnetic dipole moment**
  - **Electric quadrupole moment**
- **Mass spectrometry**

How to produce neutron-rich nuclei

Fragmentation (~100 MeV/*A*)

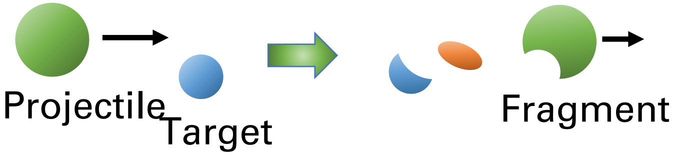

RIBF, FRIB, FAIR, …

Subtractive

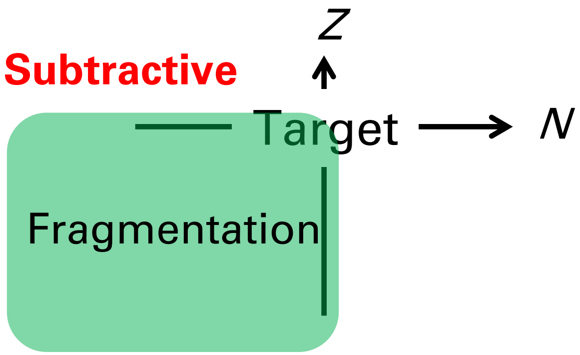

Access to the lower left direction.

Fusion (~5 MeV/*A*)

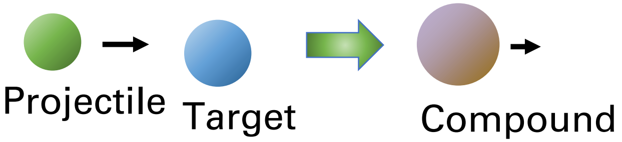

GARIS, SPIRAL2 S³, …

Additive

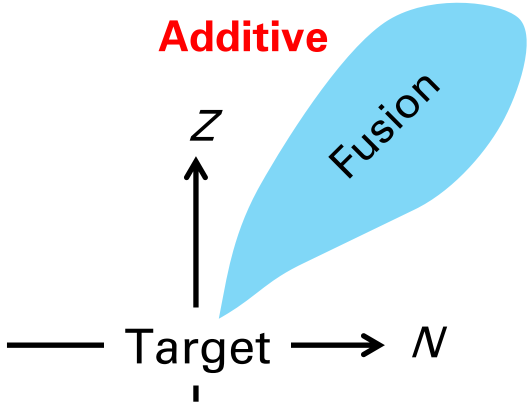

Access to the upper right direction.

Multinucleon transfer (5 – 10 MeV/*A*)

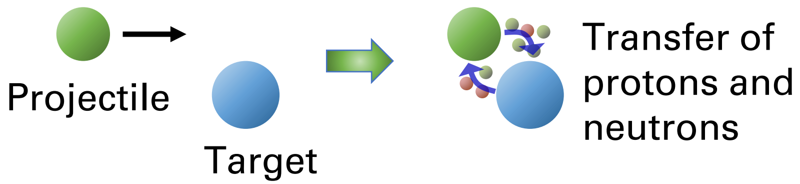

Additive & Subtractive

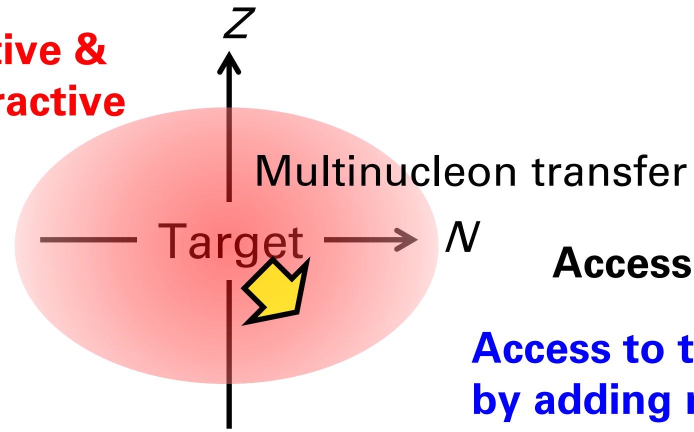

Access to all direction.

Access to the lower right direction by adding neutrons and subtracting protons.

Spectroscopy of neutron-rich nuclei around *N*=126 and beyond

r-process nucleosynthesis

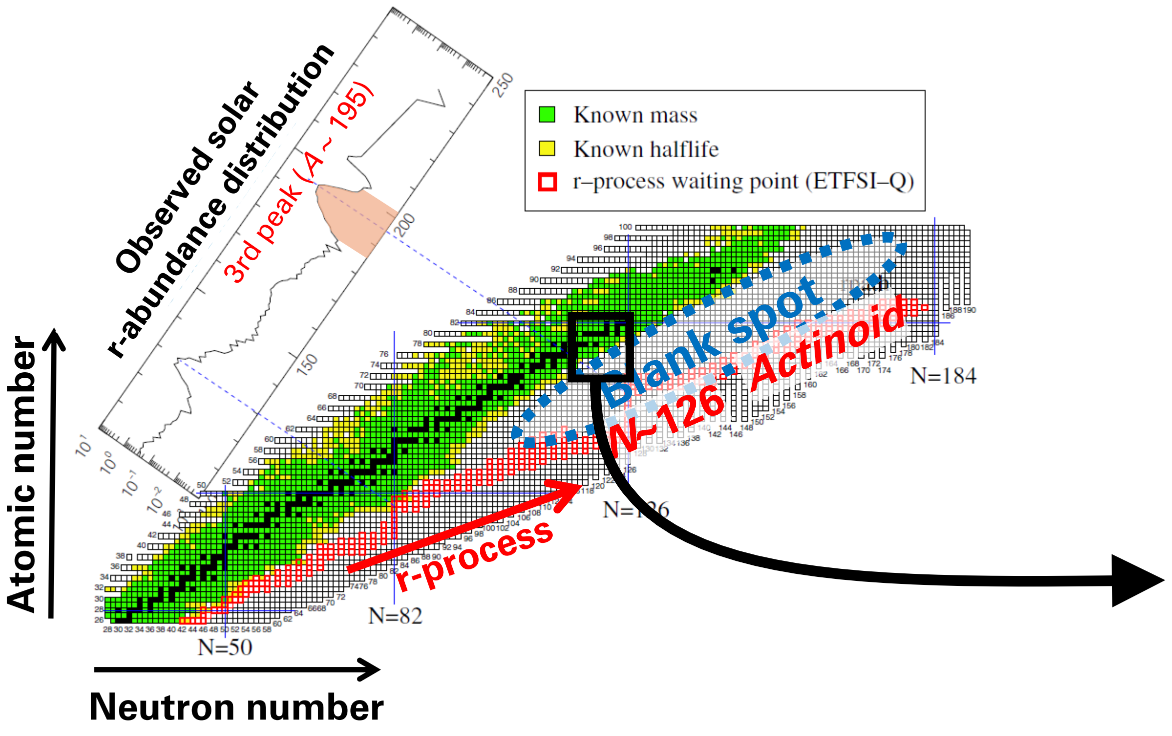

H. Grawe et al., Rept. Prog. Phys. 70, 1525 – 1582 (2007).

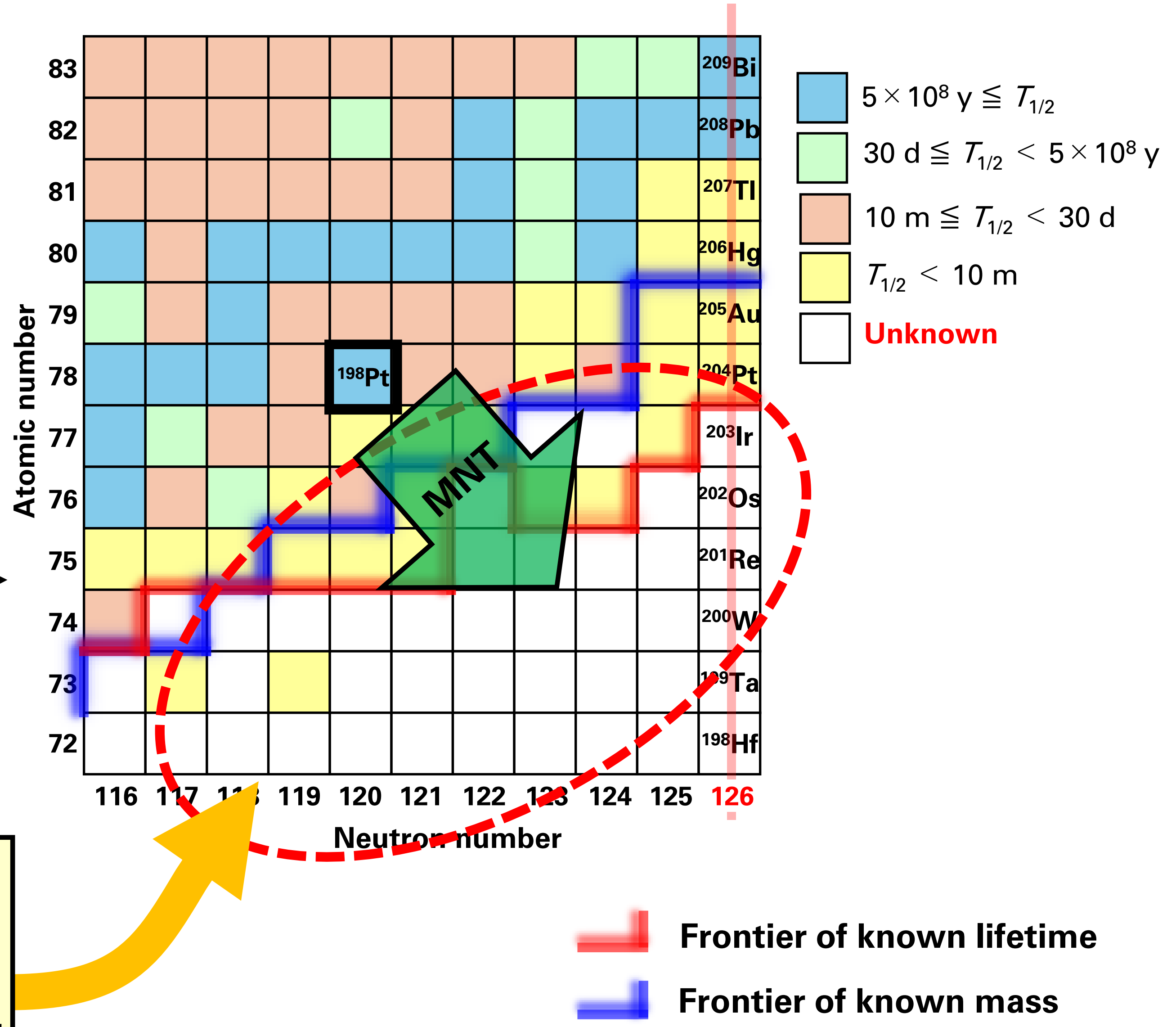

- ◆ **Decay spectroscopy**
  - ➢ **Half life**
  - ➢ **Decay scheme**
- ◆ **Laser spectroscopy**
  - ➢ **Charge radius**
  - ➢ **Magnetic dipole moment**
  - ➢ **Electric quadrupole moment**
- ◆ **Mass spectroscopy**

Low energy heavy ion reactions

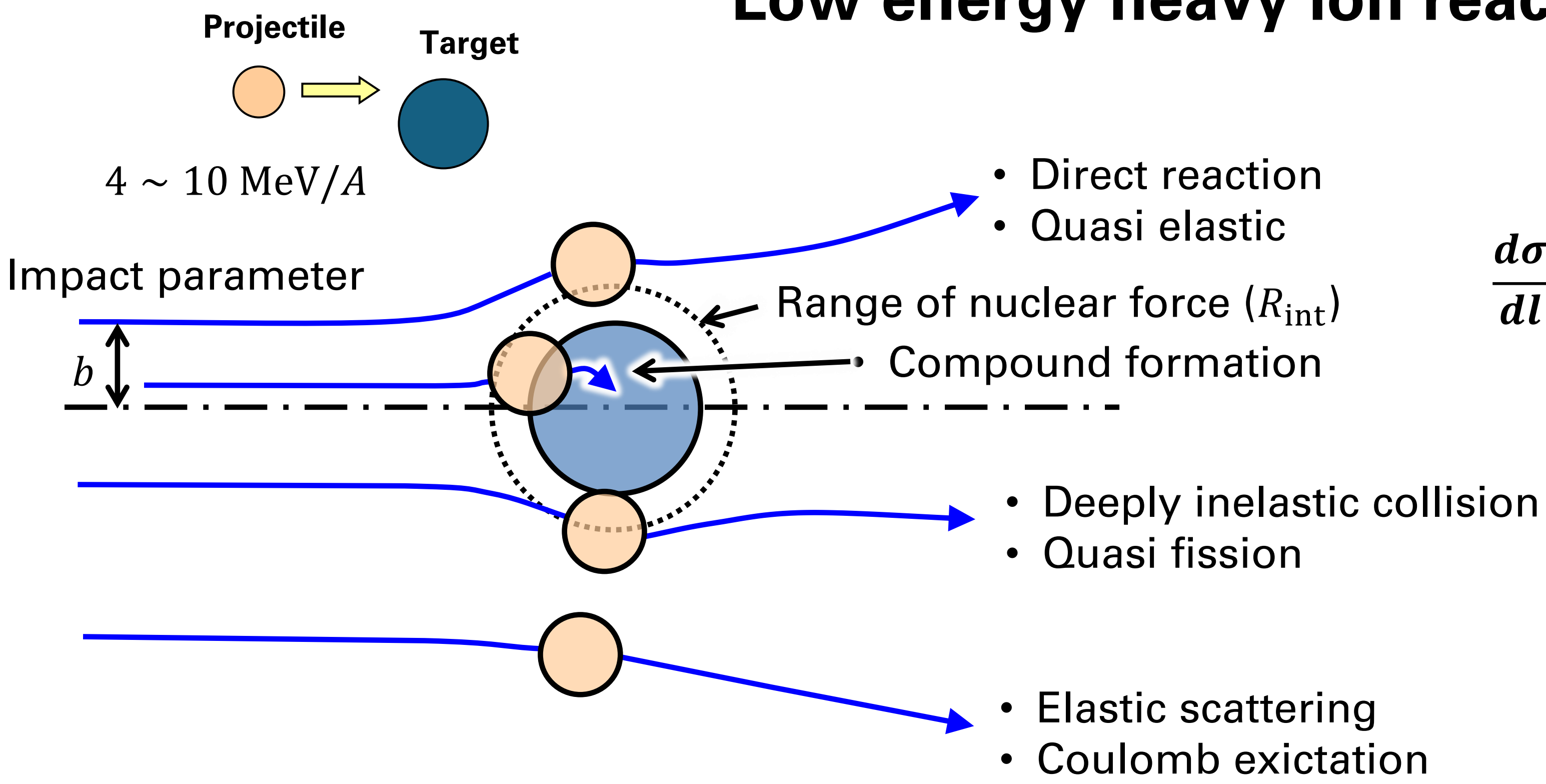

Cross section

$$\sigma = \pi b^2 = \pi \left(\frac{L}{\mu v}\right)^2 = \pi \left(\frac{\hbar}{\mu v}\right)^2 l(l+1) = \frac{1}{4\pi}\lambda^2 l(l+1)$$

λ : de Broglie wavelength
l : Orbital angular momentum quantum number

Differential cross section with respect to orbital angular momentum

$$\frac{d\sigma}{dl} = \frac{1}{2\pi}\lambda^2\left(l+\frac{1}{2}\right)$$

Differential cross section with respect to orbital angular momentum

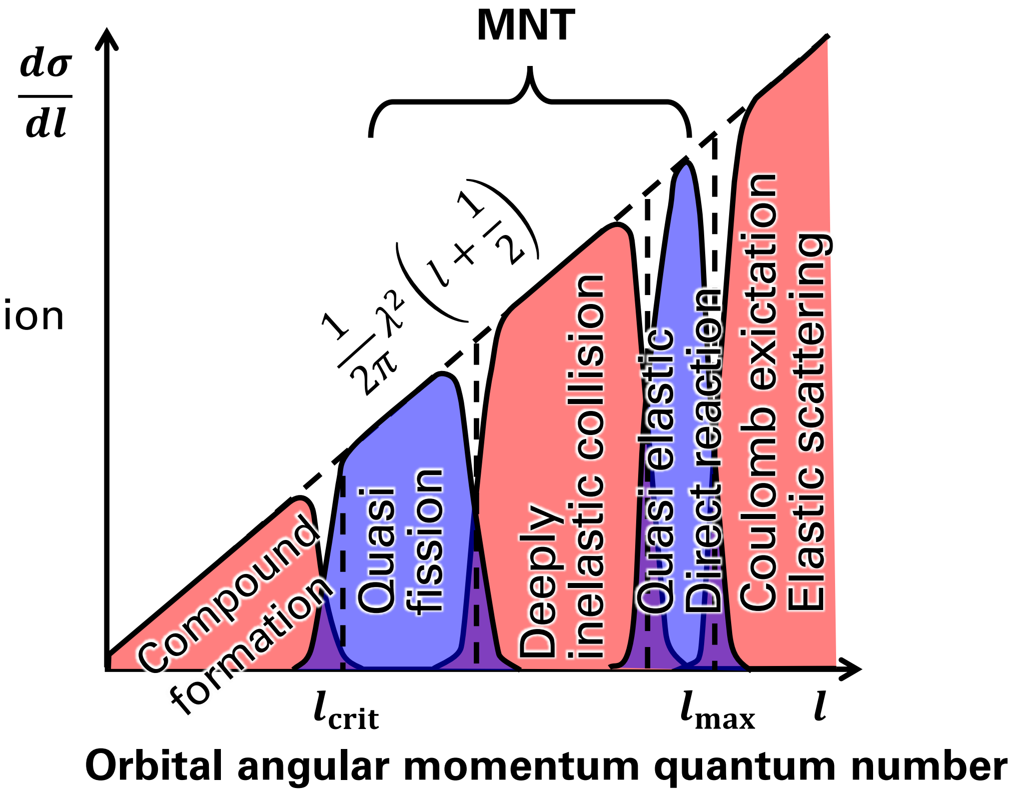

Light ion (p, d, α) reactions

- Direct reaction
- Fusion reaction

MNT reactions for neutron-rich nuclei around $N = 126$

The feasibility of the MNT reactions to produce neutron-rich nuclei was studied in the reaction system of ^{136}Xe (8 MeV/A) + ^{198}Pt (1.3 mg/cm^2).

Projectile-like fragments (PLFs) were detected by VAMOS++, and target-like fragment (TLF) distributions were deduced.

Y.X. Watanabe et al., Phys. Rev. Lett. 115, 172503 (2015).

Isotopic distributions of target-like fragments (TLFs)

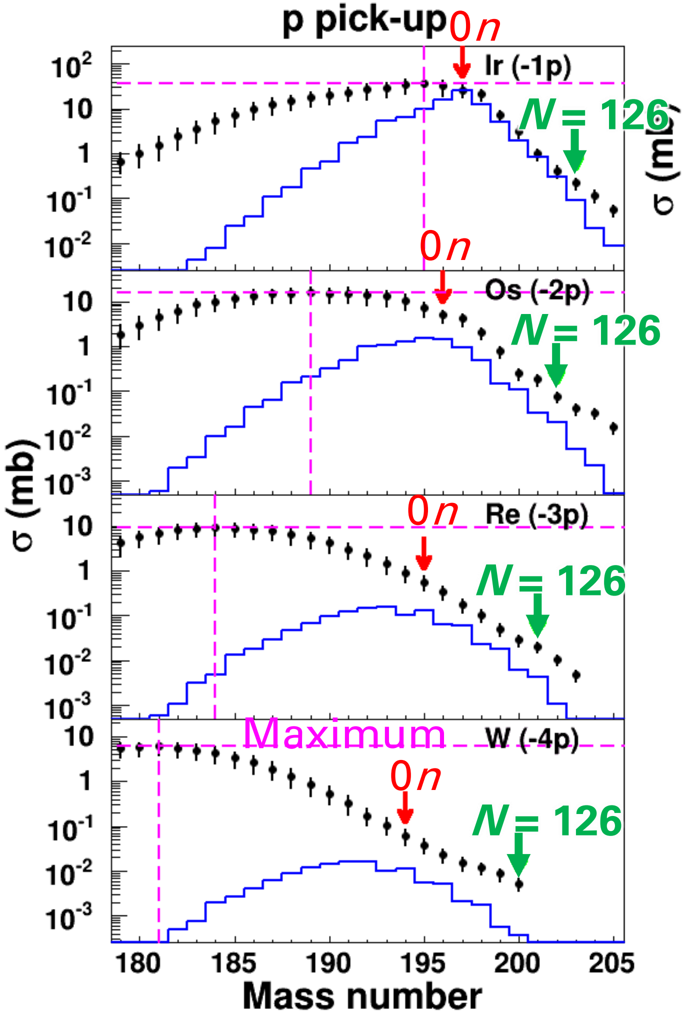

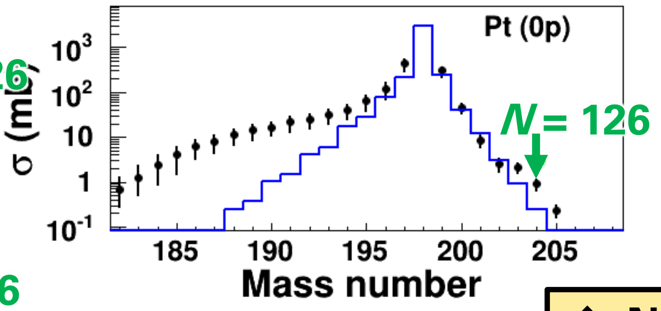

- Measurements
- *GRAZING calculations*

A. Winther et al., Nucl. Phys. A 572, 191 (1994); 594, 203 (1995).

- **Neutron-deficient side**
  - Large discrepancy between the measurements and the GRAZING calculations.
  - It is because of strongly damped component with N/Z equilibration, which is not included in the GRAZING calculations.
- **Neutron-rich side ($N \sim 126$)**
  - Contributed by the weakly damped component with less particle evaporation.
  - The GRAZING calculations, which include particle evaporation, show relatively good agreement with the measurements.

Properties of MNT reactions

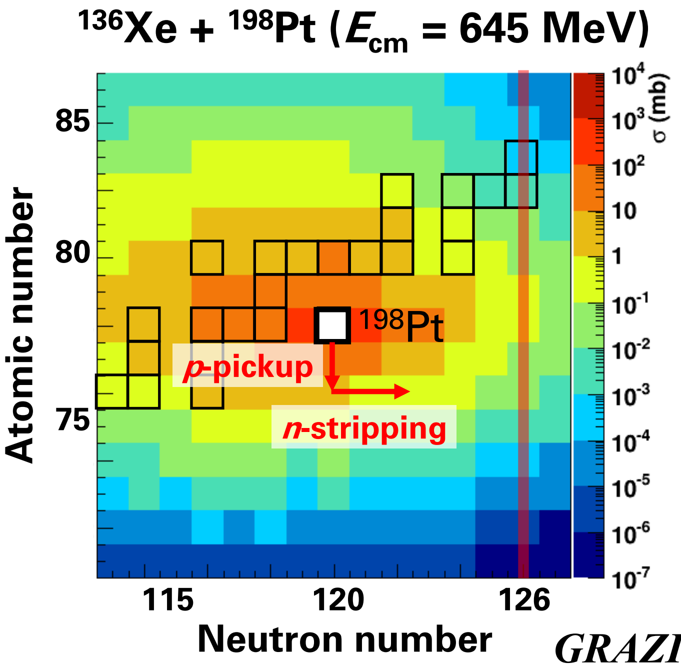

GRAZING calculations

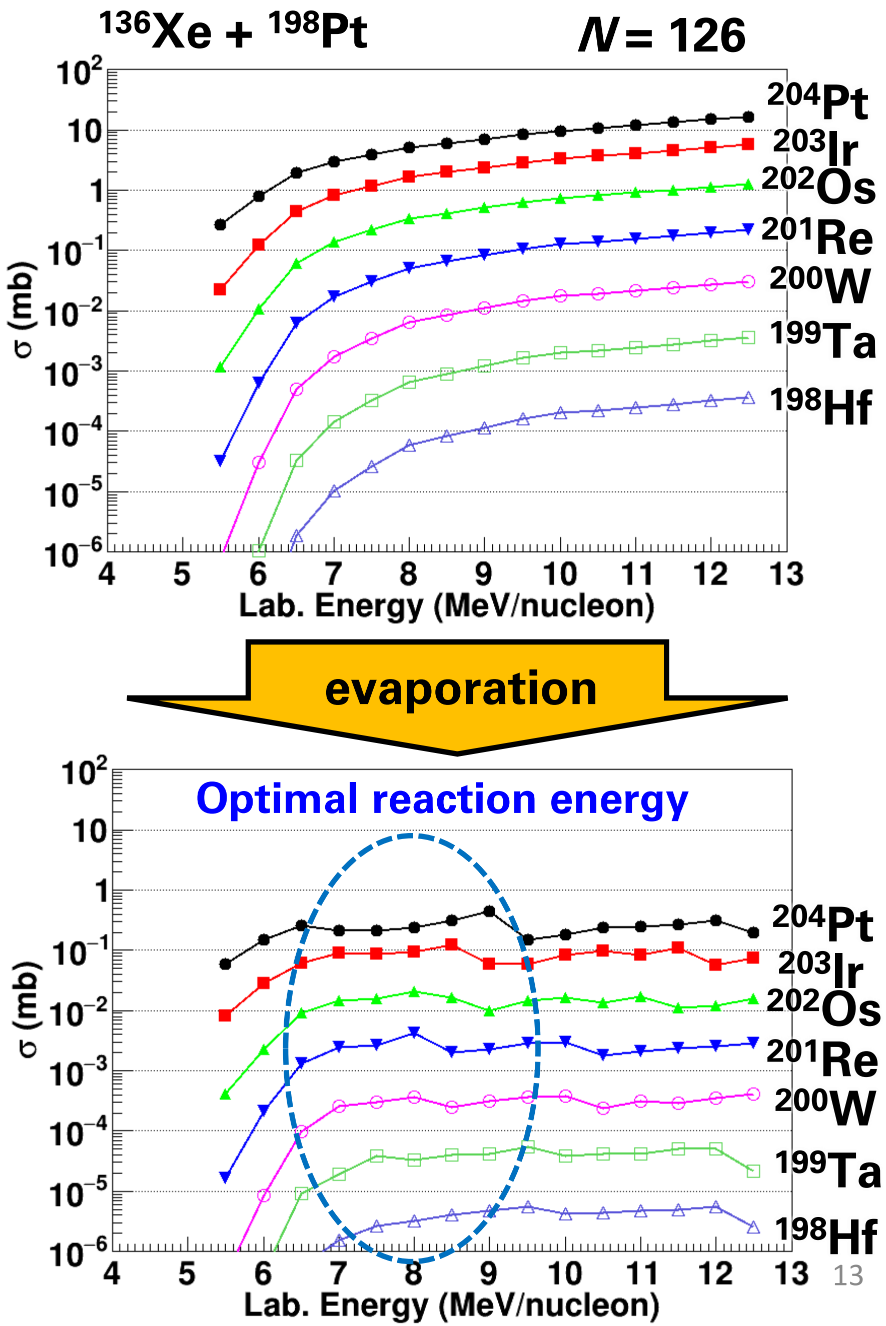

> Experimental difficulty
> - Simultaneous production of numerous nuclides → background

Properties of MNT reactions

$^{136}Xe + ^{198}Pt$ (E_{cm} = 645 MeV)

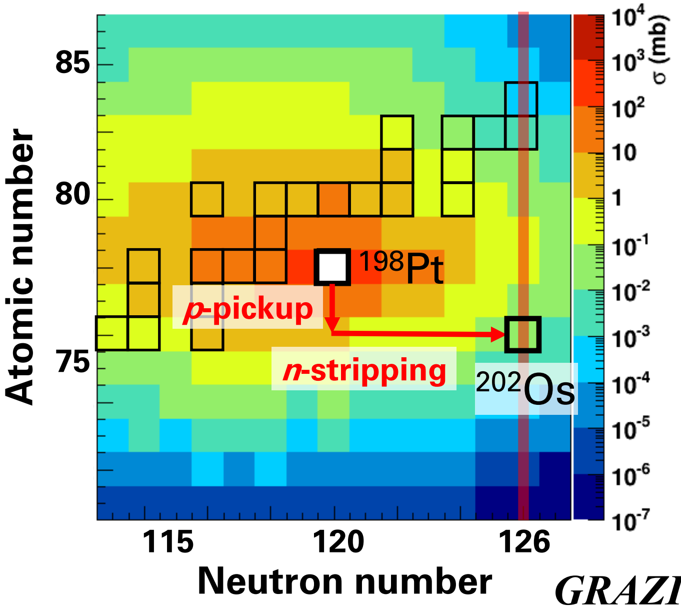

GRAZING calculations

MNT reaction of

^{136}Xe (9.4 MeV/nucleon) + ^{198}Pt (12.5 mg/cm^2)

Energy-angle distribution

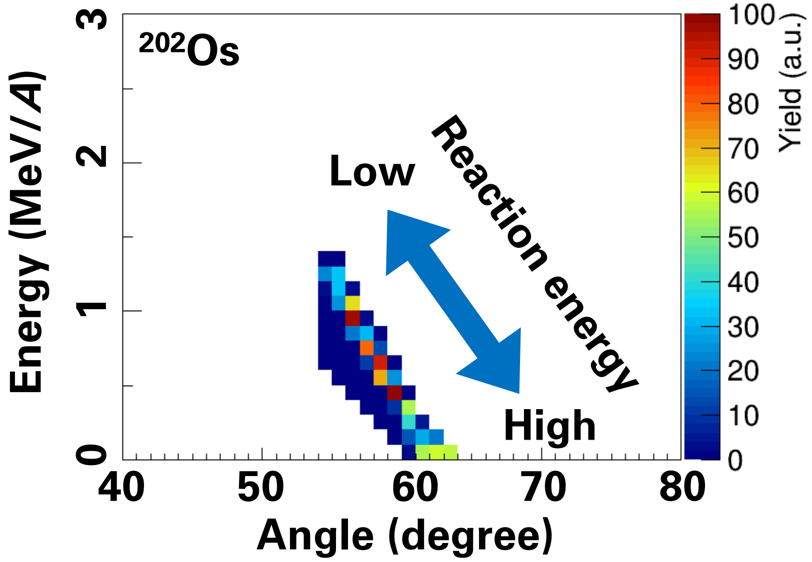

Experimental difficulty

- Simultaneous production of numerous nuclides → background
- Low and wide energy distribution
- Wide angular distribution around the grazing angle

Development of experimental techniques to collect, separate, and identify reaction products.

Energy distribution

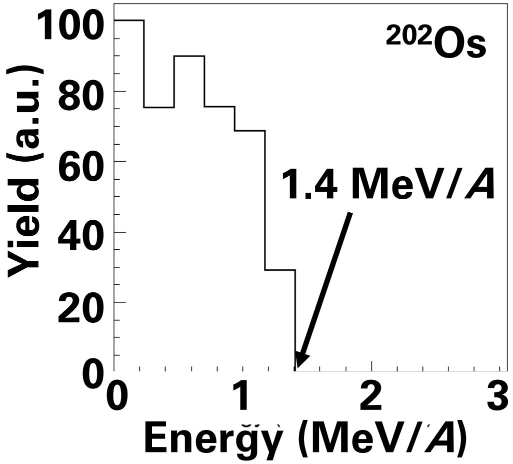

Angular distribution

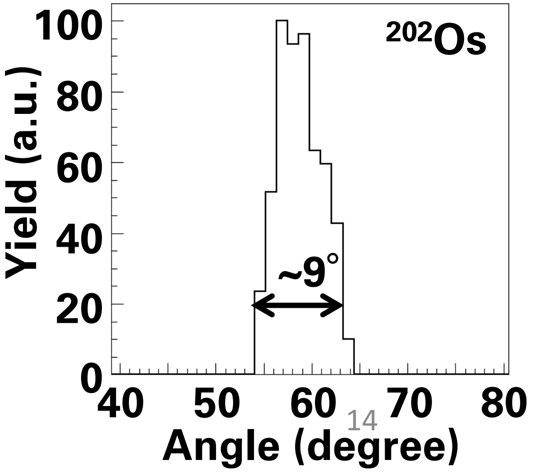

RIKEN RIBF (RI Beam Factory)

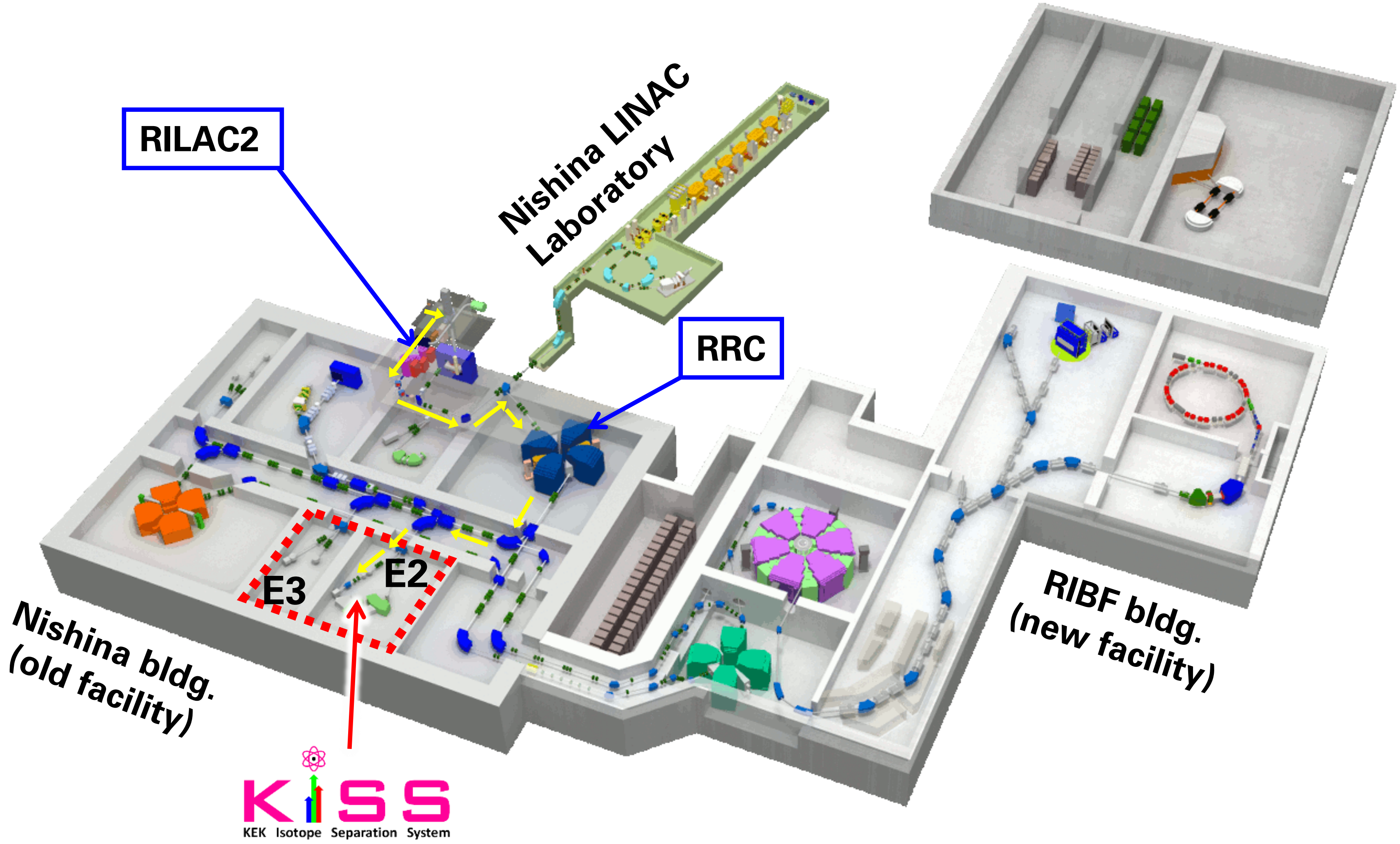

KEK Isotope Separation System

Heavy ion beams (^{136}***Xe,*** ^{238}***U, …),* 10.75 MeV*/ nucleon,* ≲ *100 pnA***

KEK Isotope Separation System (KISS)

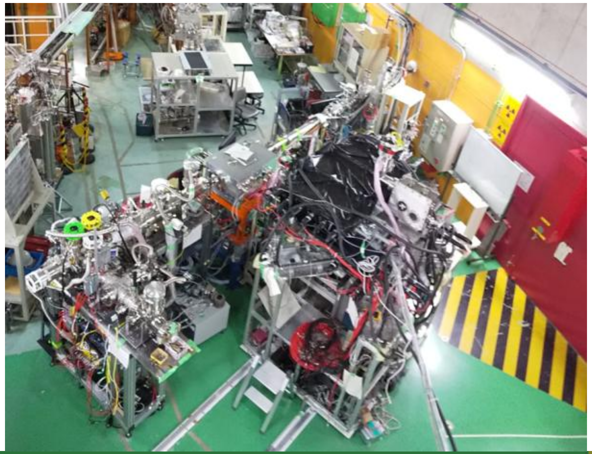

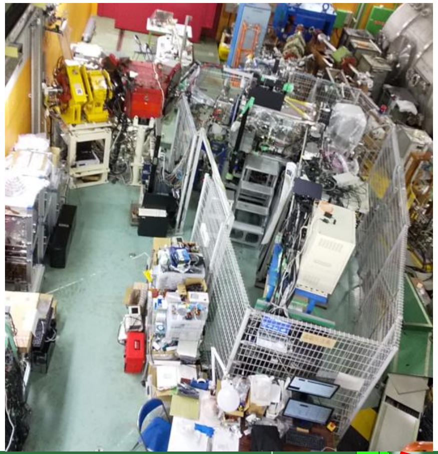

KISS
KEK Isotope Separation System

2009: KISS project started
2011: KISS installed
2013: Online testing started
2015: WNSC established
2016: KISS has been open for users

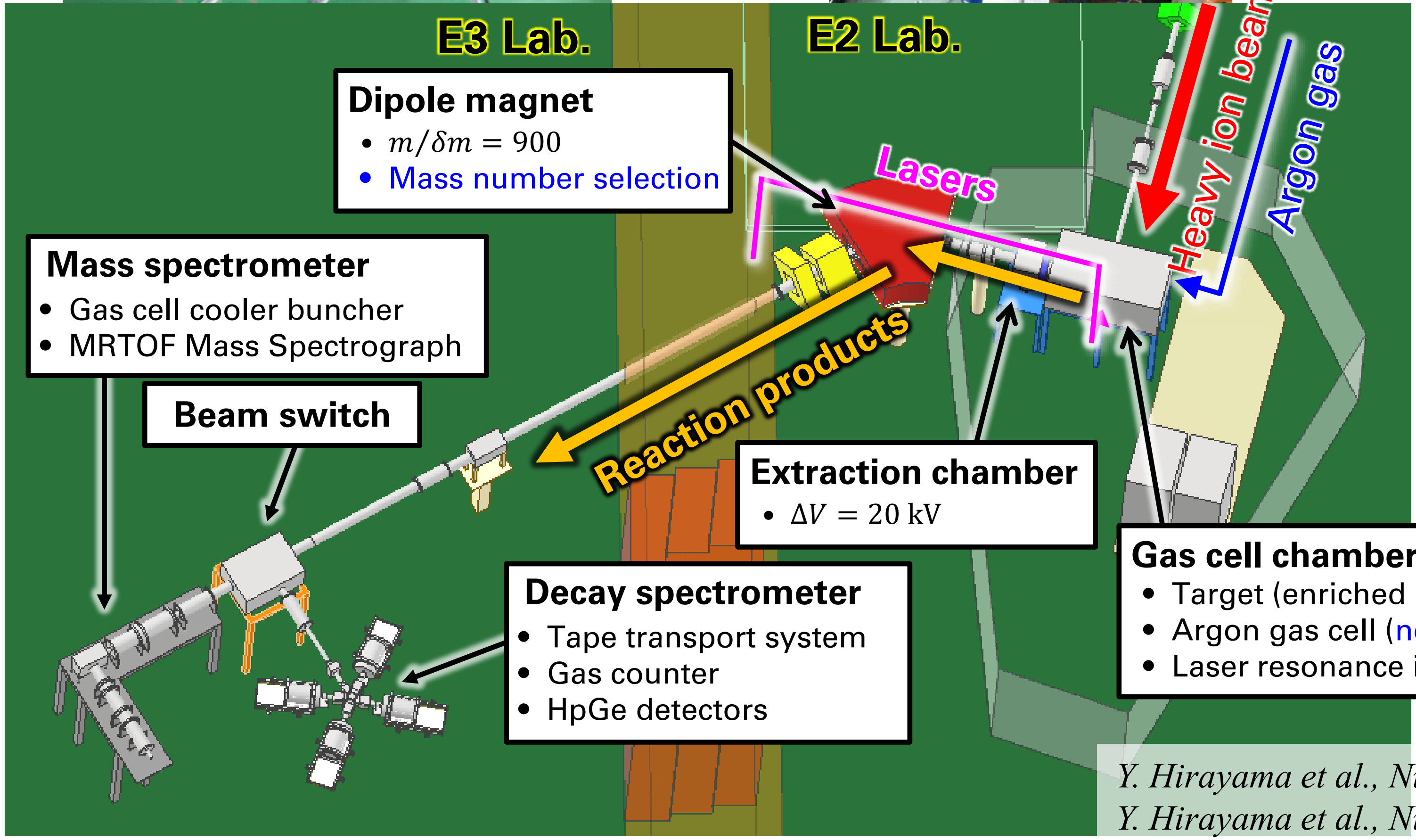

Y. Hirayama et al., Nucl. Instrum. and Meth. B 353, 4 – 15 (2015),
Y. Hirayama et al., Nucl. Instrum. and Meth. B 412, 11 – 18 (2017).

Production, collection, and separation

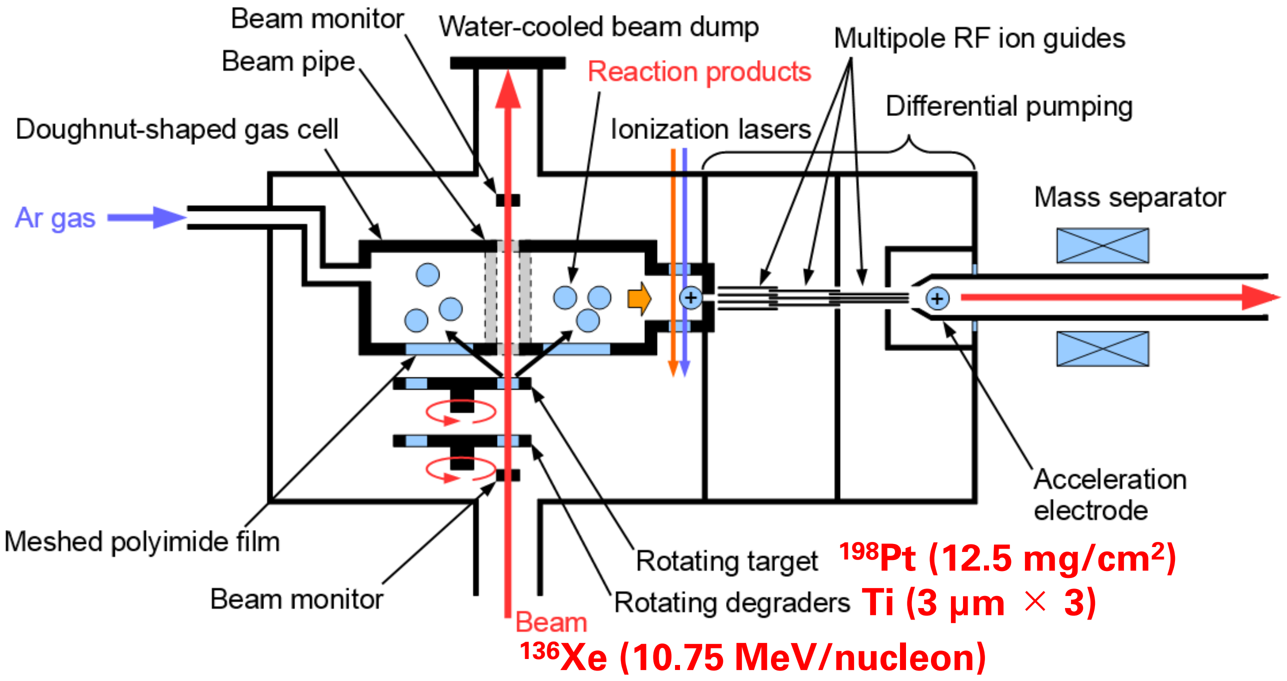

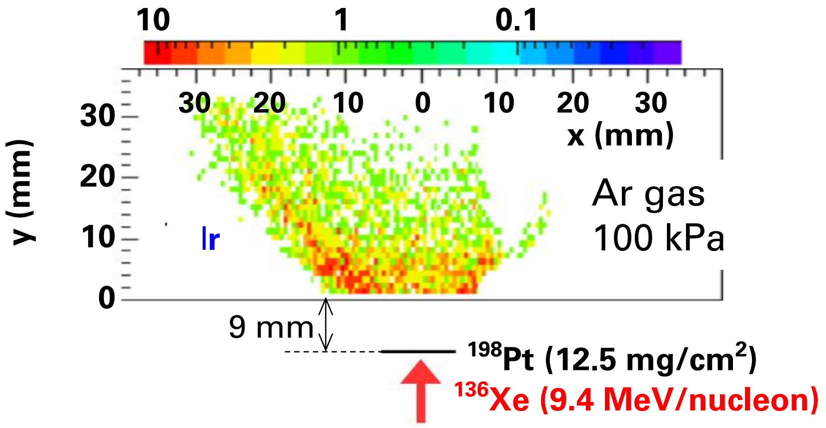

Doughnut-shaped argon gas cell

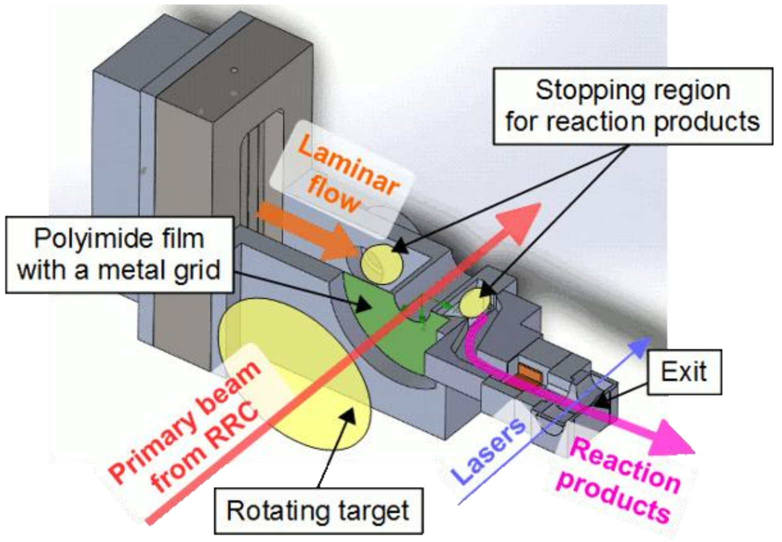

- Nuclear production by multinucleon transfer (MNT) reactions
- Efficient collection of reaction products by gas cell
- Neutralization in argon gas
- Element selection by laser resonance ionization
- Mass selection by dipole magnet

Y. Hirayama et al., Nucl. Instrum. and Meth. B 412, 11 – 18 (2017).

Decay spectroscopy

MSPGC
(Multi-Segmented Proportional Gas Counter)

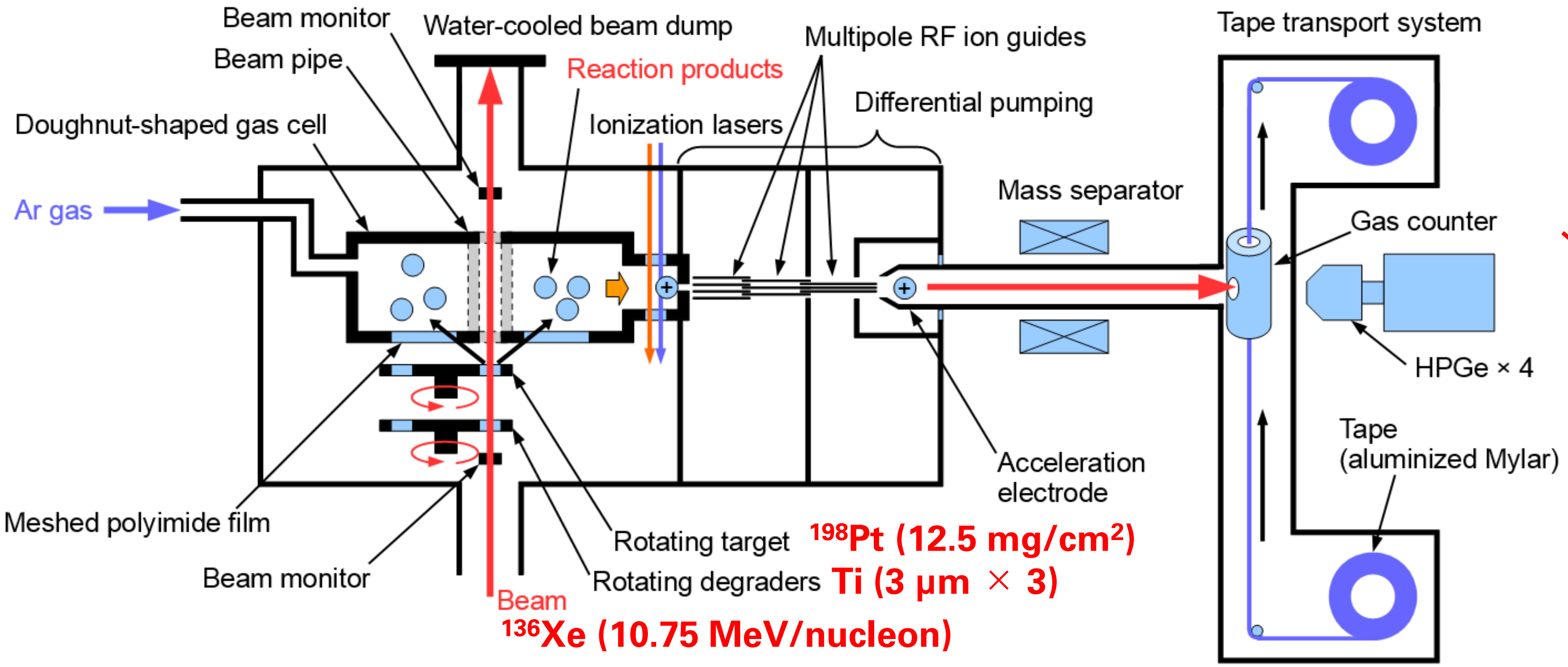

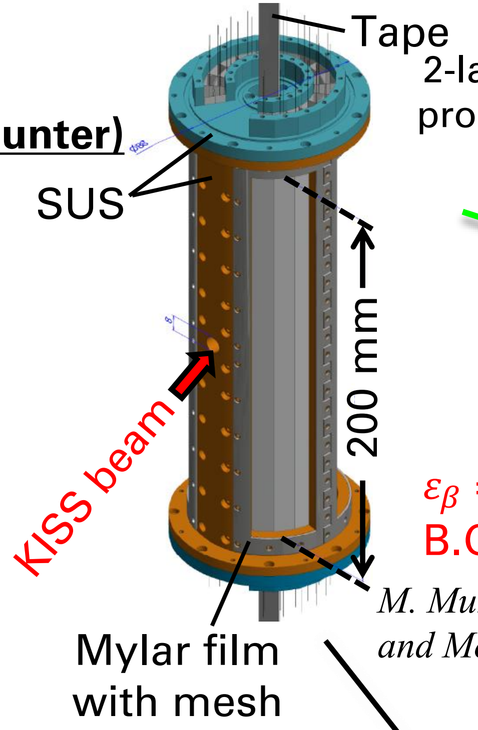

2-layered 16-segmented proportional gas counter

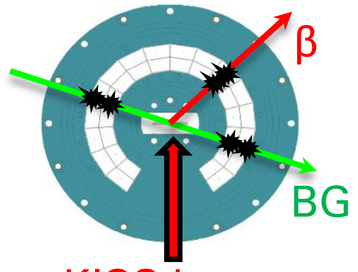

ε_β = 40% for Q_β = 1 MeV
B.G. rate = 0.1 cps

M. Mukai et al., Nucl. Instrum. and Methods A 884, 1–10 (2018).

Four HPGe (High-Purity Germanium) clover detectors

ε_γ = 10% for E_γ = 1 MeV

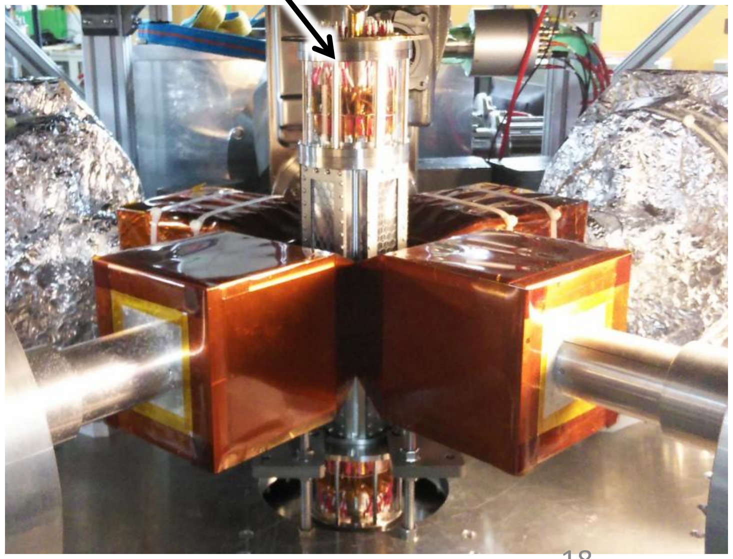

Collaboration with IBS (Korea), IMP (China)

Mass spectrometry

MRTOF-MS (Multi-Reflection Time-Of-Flight Mass Spectrograph)

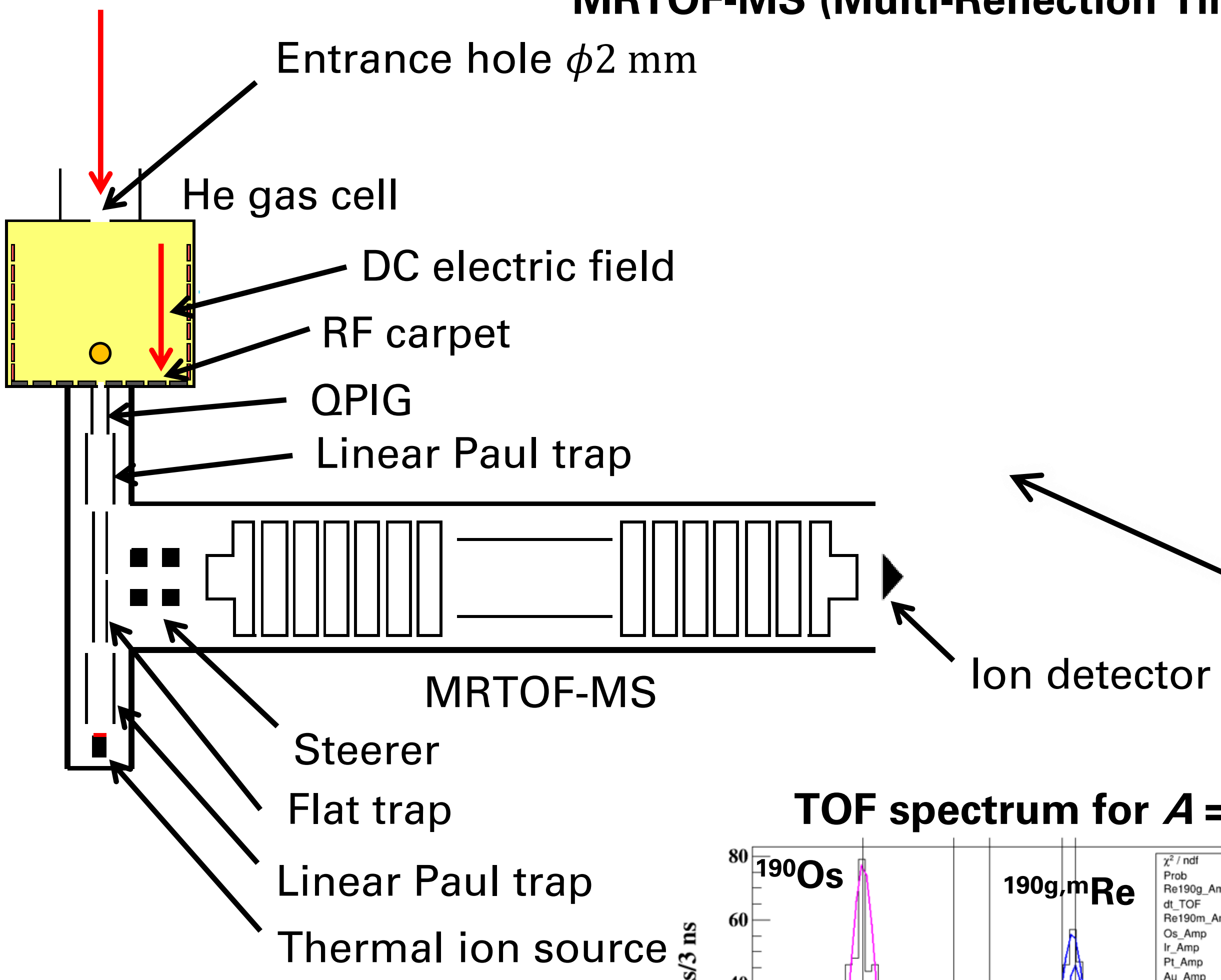

Measurement time: a few 10 ms
Mass resolving power: > 400 000
Efficiency: ~3%

TOF spectrum for $A = 190$

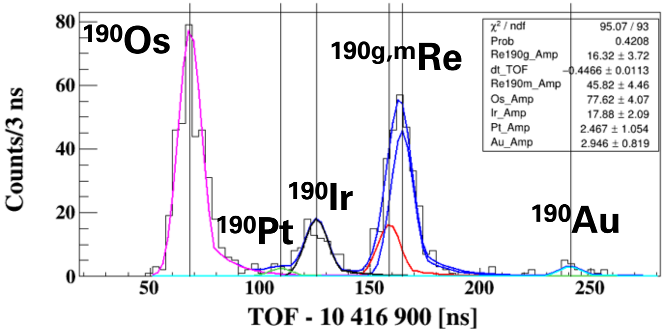

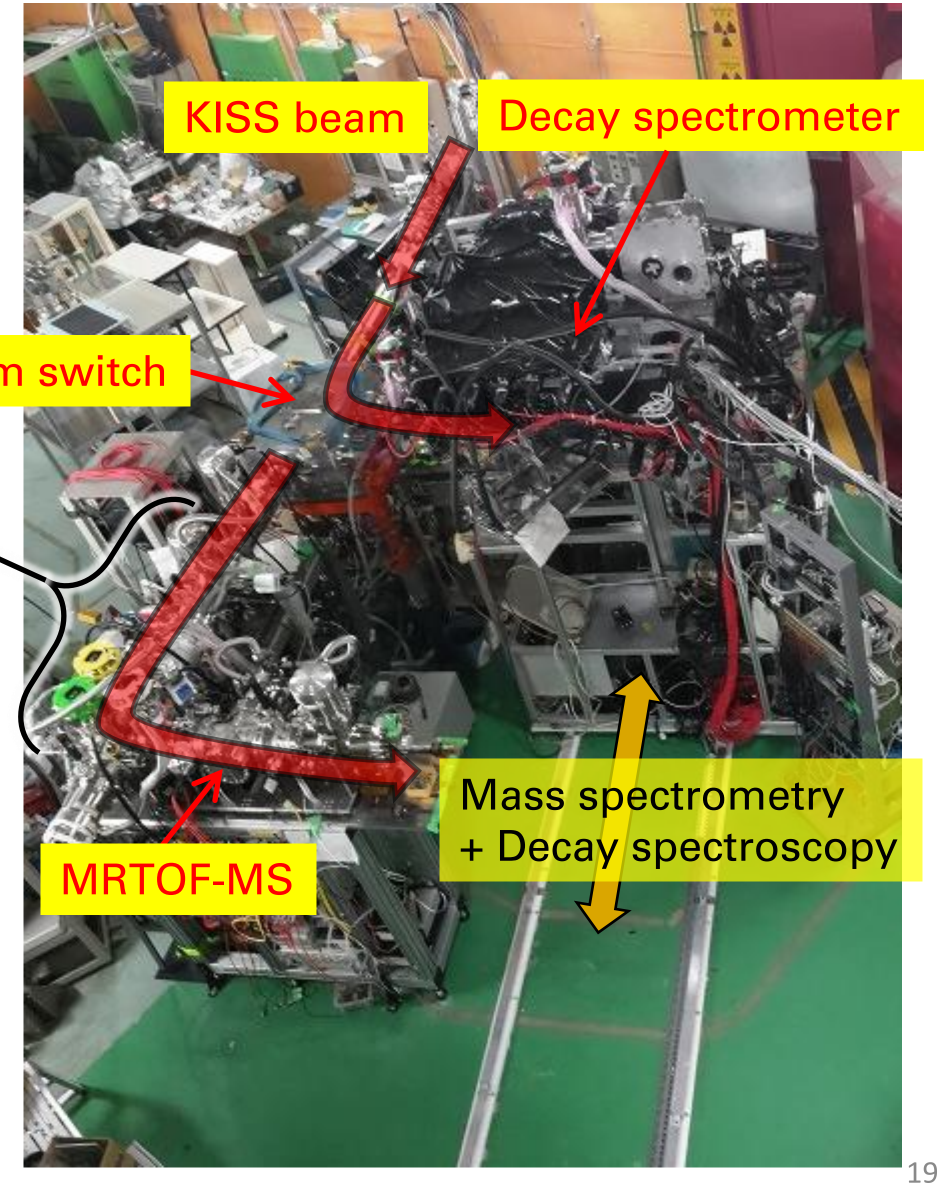

Experimental results (*N* ~ 126)

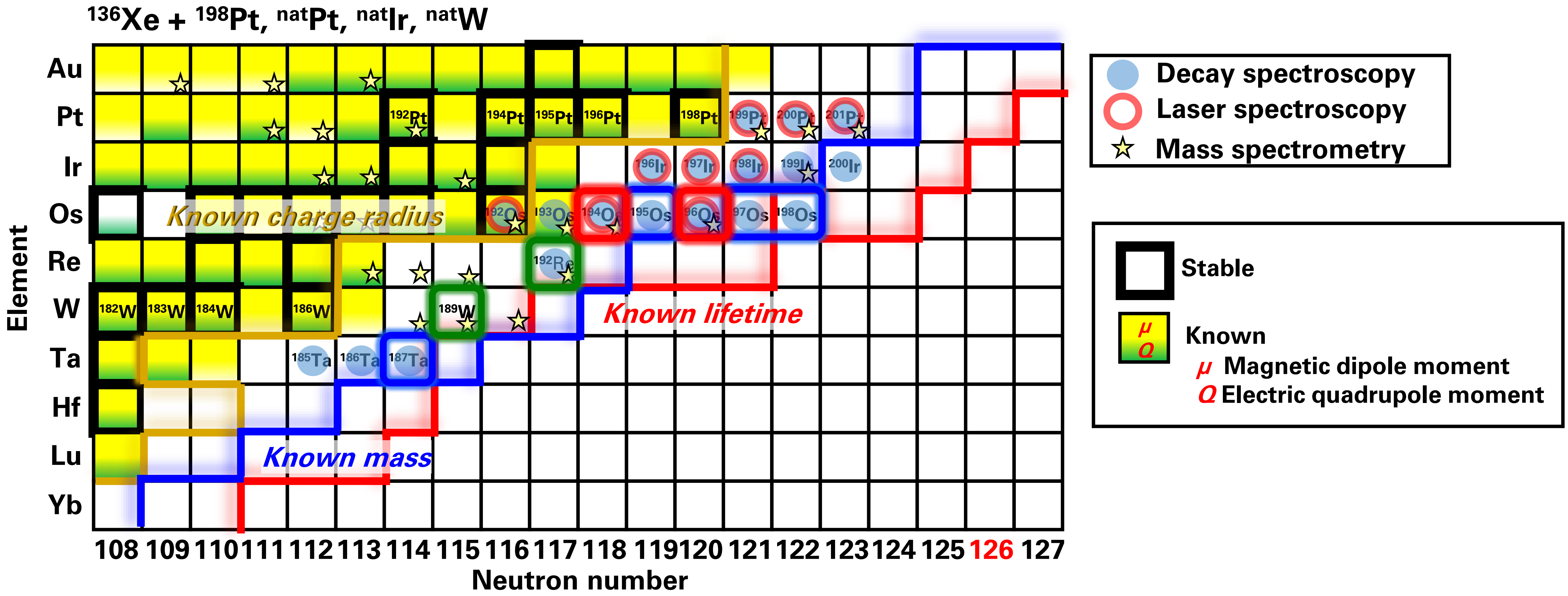

Decay spectroscopy / **Laser spectroscopy** / **Mass spectrometry**

^{189}W, ^{192}Re : *M. Mukai et al., Phys. Rev. C 111, 014322 (2025).*

^{187m2}Ta : *J.L. Chen et al., Phys. Rev. C 111, 014304 (2025).*

$^{200-201}$Pt: *Y. Hirayama et al., Phys. Rev. C 106, 034326 (2022).*

^{187g}Ta: *M. Mukai et al., Phys. Rev. C 105, 034331 (2022).*

^{186m}Ta: *Y.X. Watanabe et al., Phys. Rev. C 104, 024330 (2021).*

^{195g}Os: *M. Ahmed et al., Phys. Rev. C 103, 054312 (2021).*

^{195m}Os: *Y.X. Watanabe et al., Phys. Rev C 101, 041305(R) (2020), 103, 019902(E) (2021).*

^{192g}Re: *H. Watanabe et al., Phys. Lett. B 814, 136088 (2021).*

^{187m}Ta: *P. Walker et al., Phys. Rev. Lett. 125, 192505 (2020).*

$^{196-198}$Ir: *M. Mukai et al., Phys. Rev. C 102, 054307 (2020).*

^{194,196}Os: *H. Choi et al., Phys. Rev. C 102, 034309 (2020).*

^{197,198}Os: *Y. Hirayama et al., Phys. Rev. C 98, 014321 (2018), 069902(E) (2022).*

^{199g,m}Pt: *Y. Hirayama et al., Phys. Rev. C 96, 014307 (2017).*

β-γ spectroscopy of ^{195}Os and ^{198}Os

Time spectrum of β-ray counts

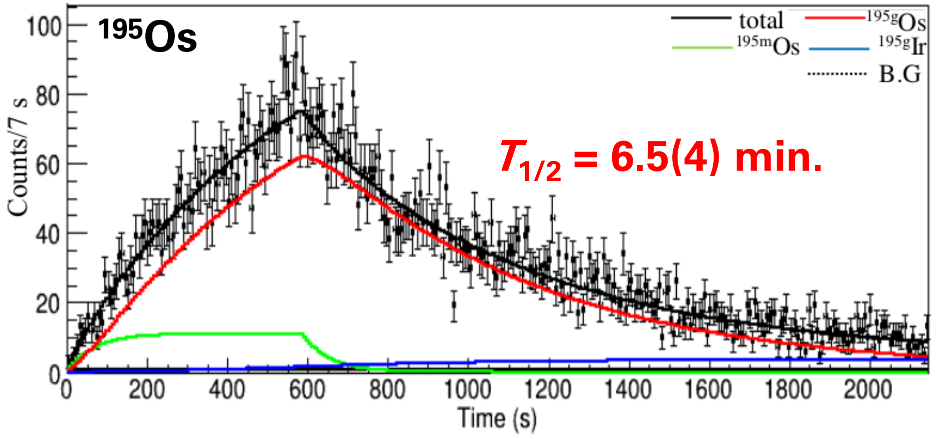

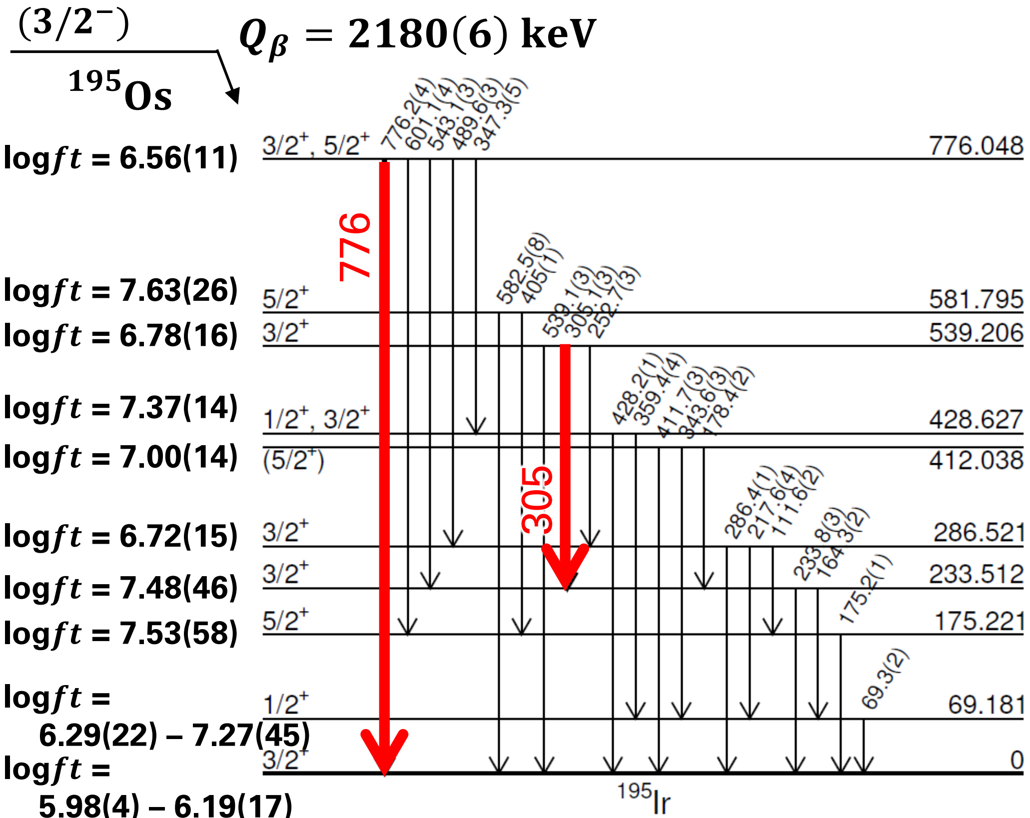

Time spectrum of β-ray counts

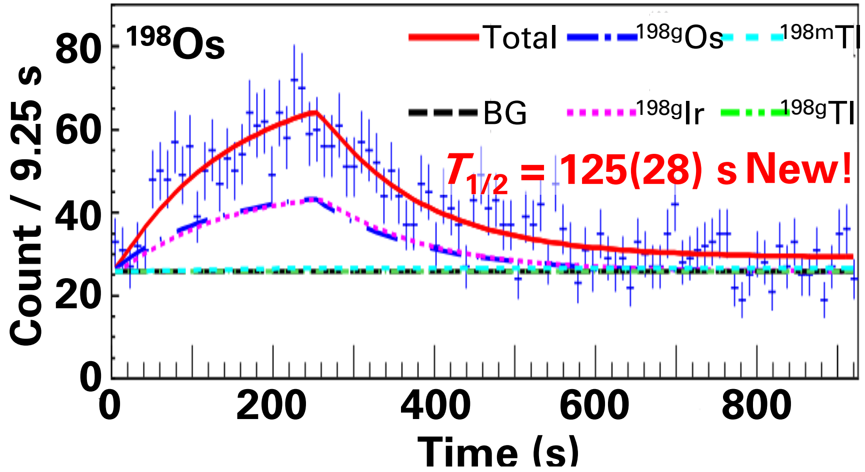

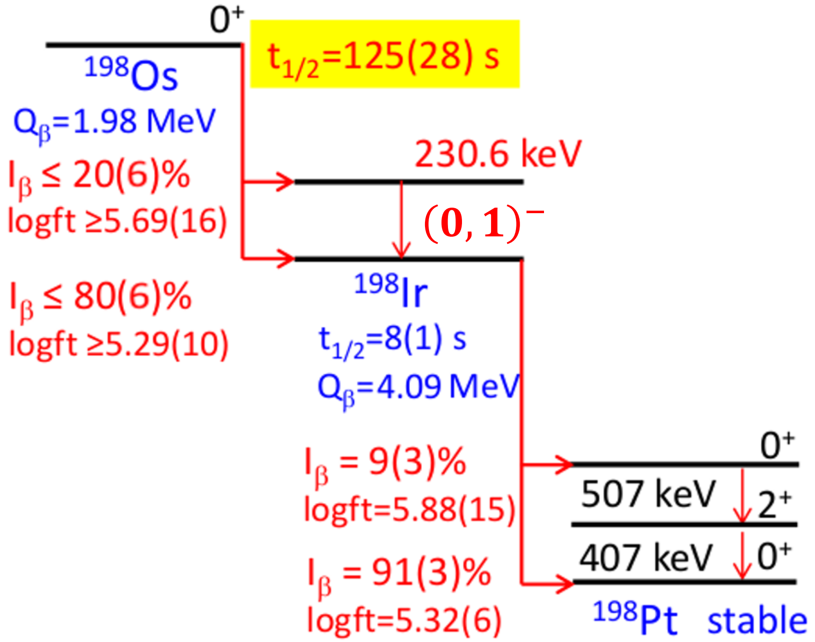

M. Ahmed et al., Phys. Rev. C 103, 054312 (2021).

Y. Hirayama et al., Phys. Rev. C 98, 014321 (2018), 106, 069902 (E) (2022).

Systematics of β-decay half-lives of osmium isotopes

Single particle levels

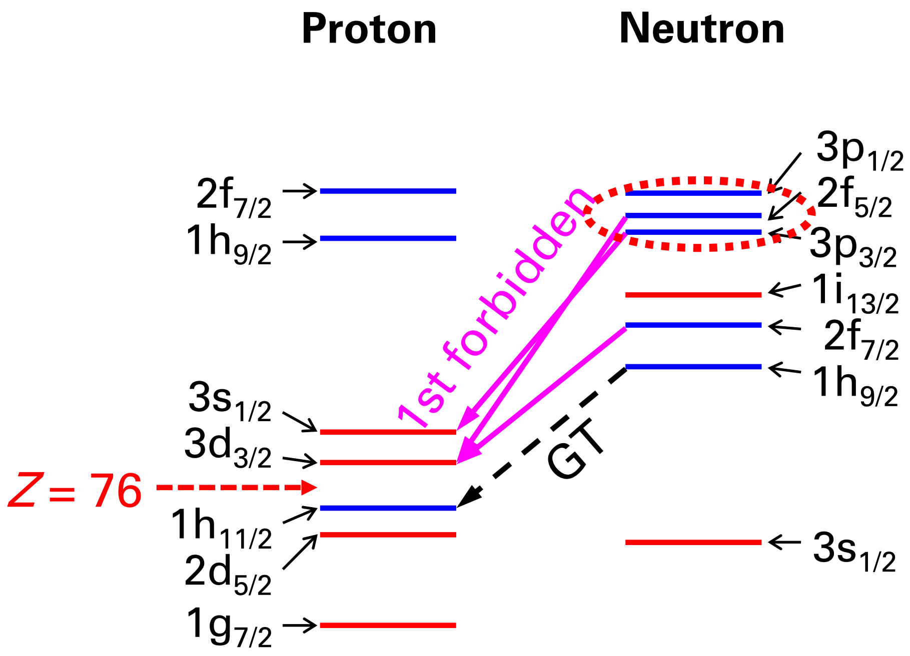

Half-lives of osmium isotopes

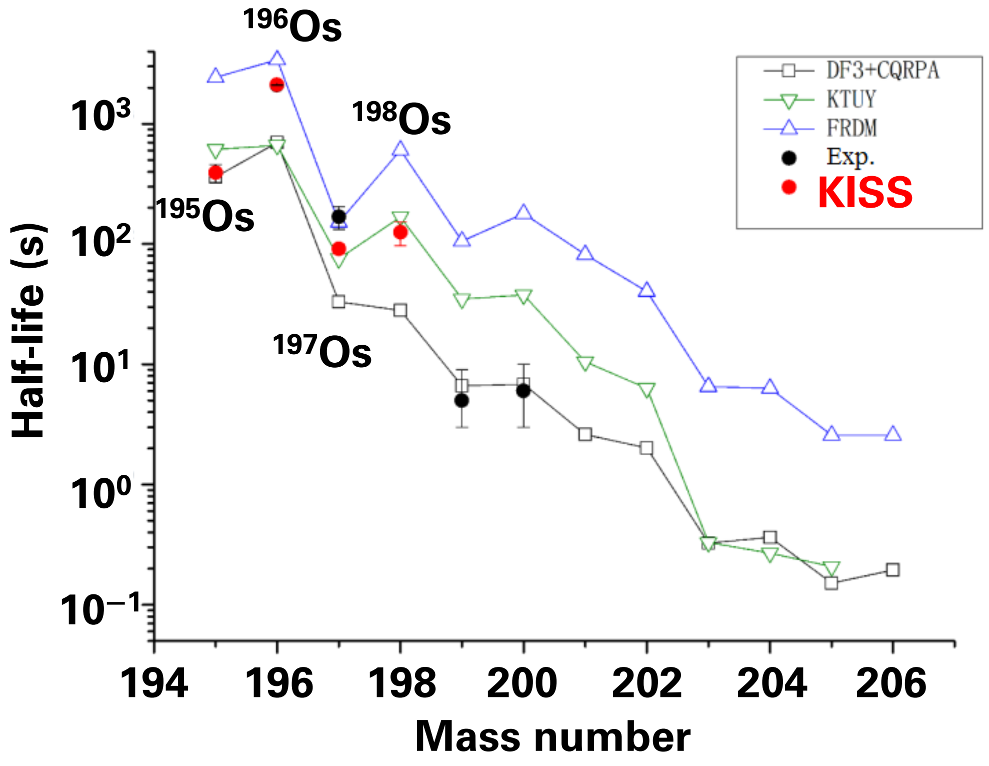

γ-ray spectroscopy of ^{187m1}Ta

Sum of γ-γ coincidence energy spectra

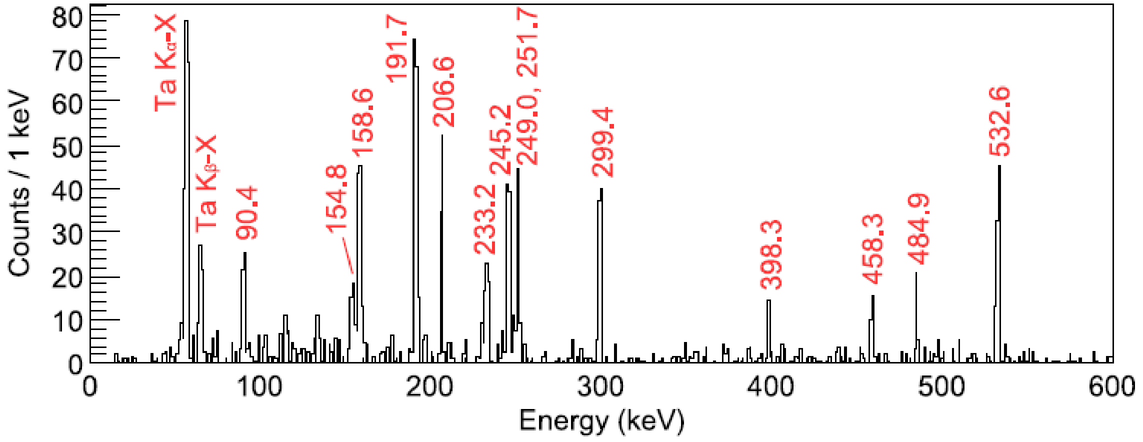

Summed time spectrum of 10 different γ–ray transitions

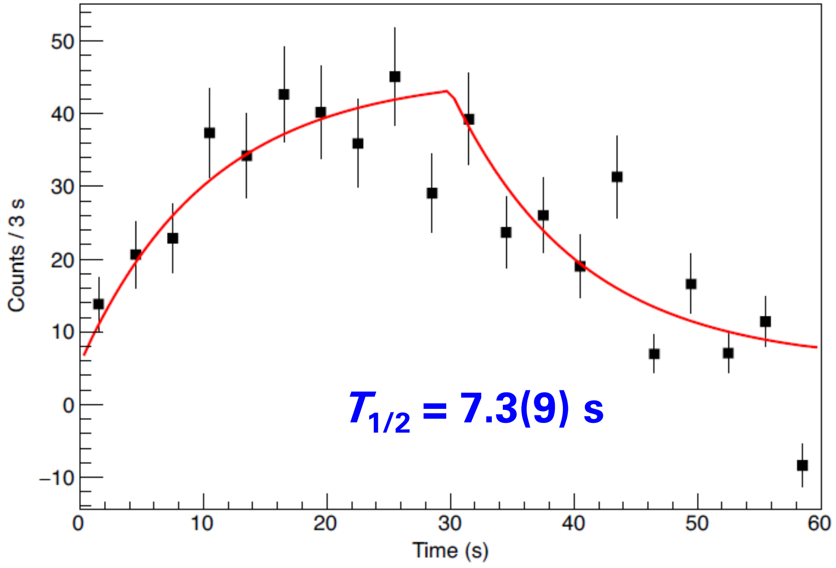

^{187m1}Ta

1778 $T_{1/2}$ = 7.3 (9) s

high-K isomer
($K = 25/2^-$)

Decay scheme of ^{187m1}Ta

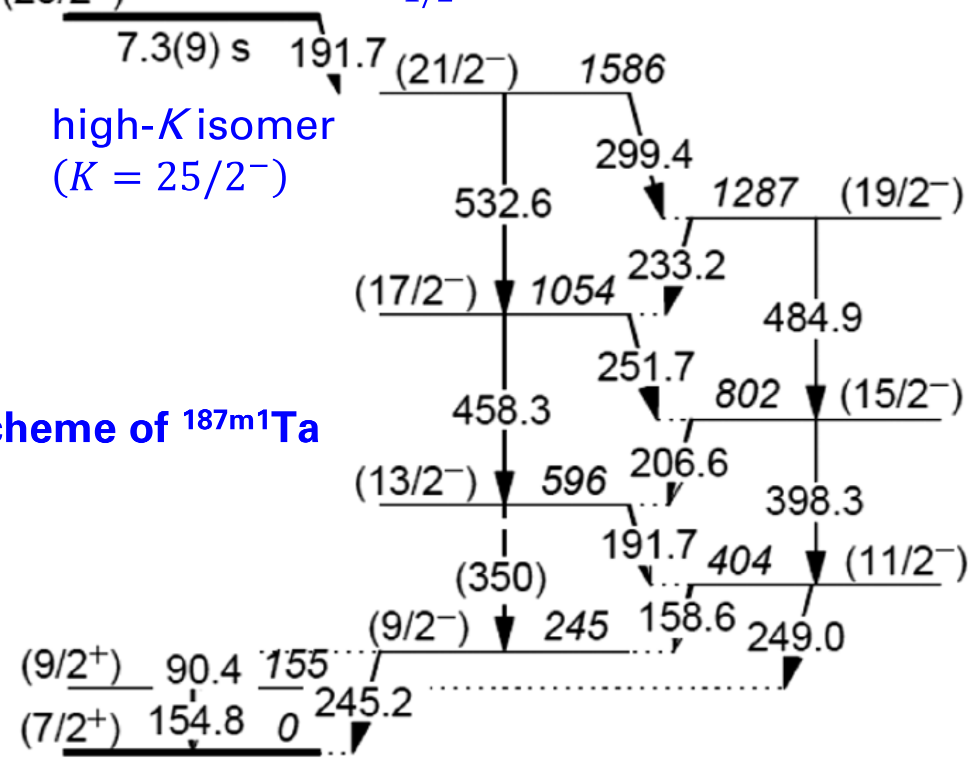

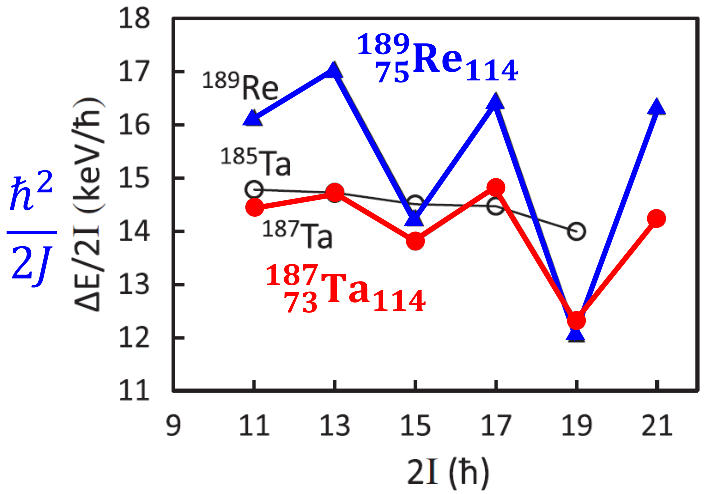

Moment of inertia in $9/2^-$ band

"As Z decreases, the β_2 deformation increases and triaxiality plays a reduced role."

P.M. Walker et al., Phys. Rev. Lett. 125, 192505 (2020).

Mass spectrometry of ^{189}W, ^{192}Re

MRTOF time spectra

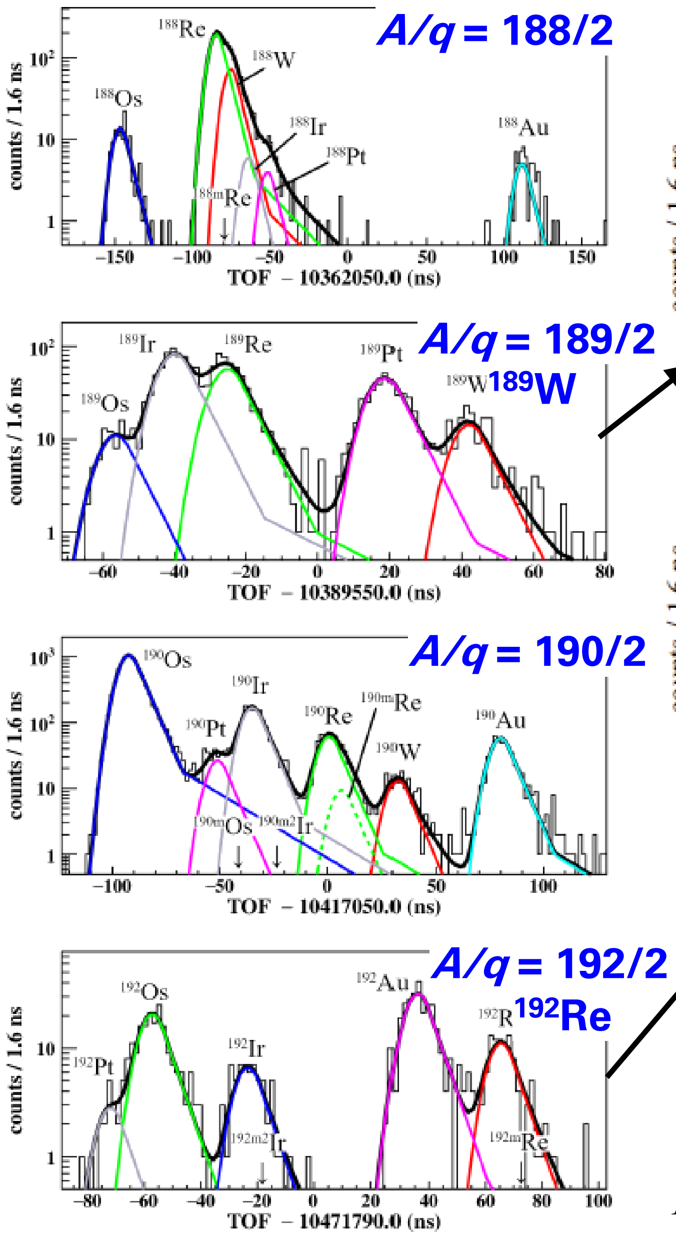

Laser resonance ionization

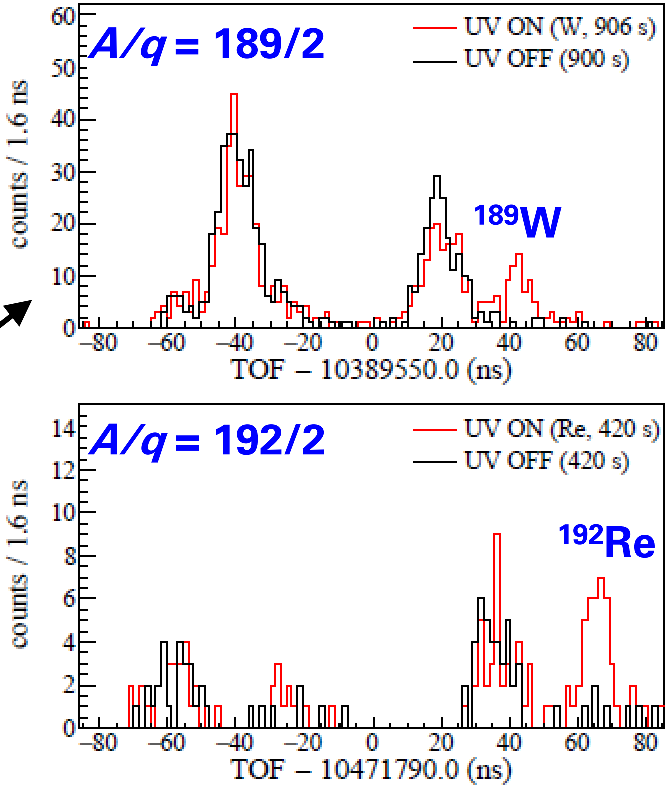

M. Mukai et al., Phys. Rev. C 111, 014322 (2025).

Atomic mass deviation from AME2020

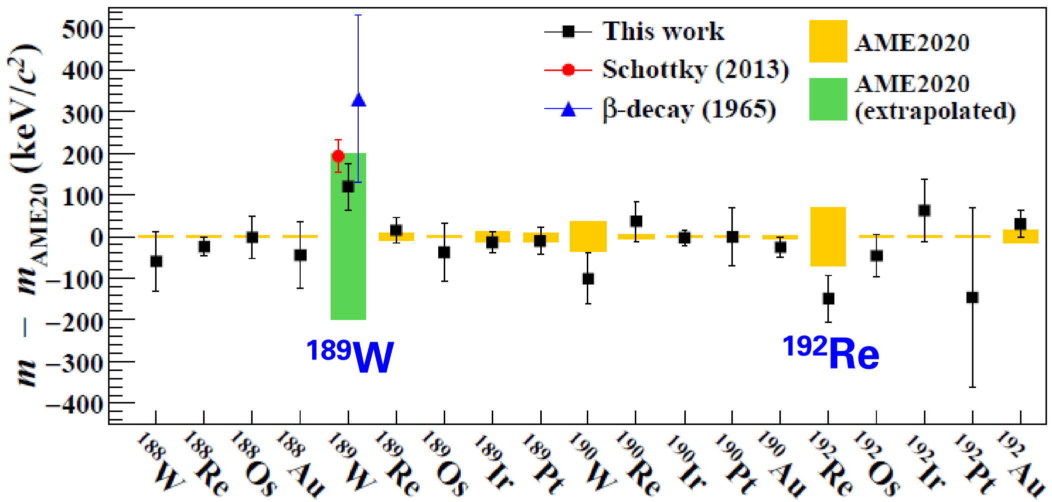

Two-neutron separation energies

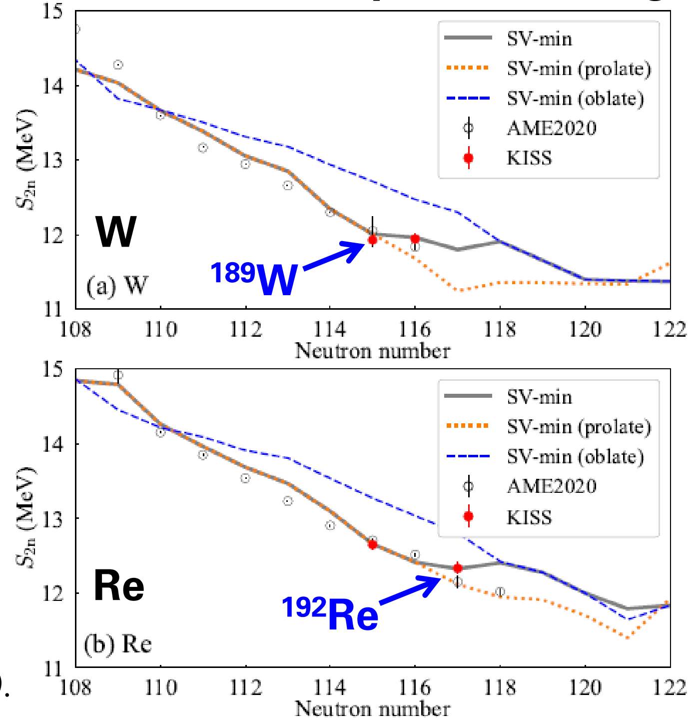

Shape transition from prolate to oblate

Laser spectroscopy of $^{194,196}Os$ with MRTOF-MS

^{194}Os $T_{1/2}$ = 6.0 years : Too long for decay count

MRTOF spectrum

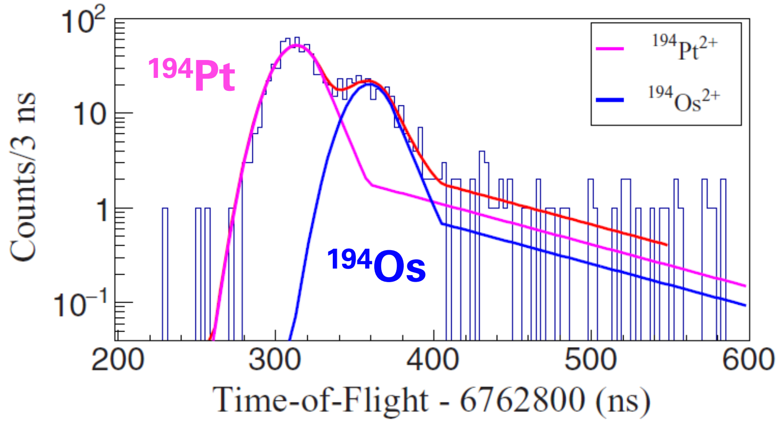

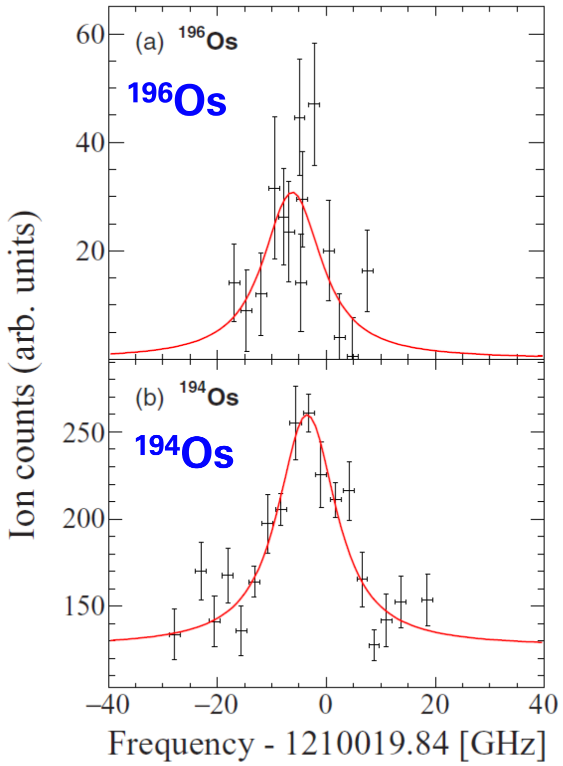

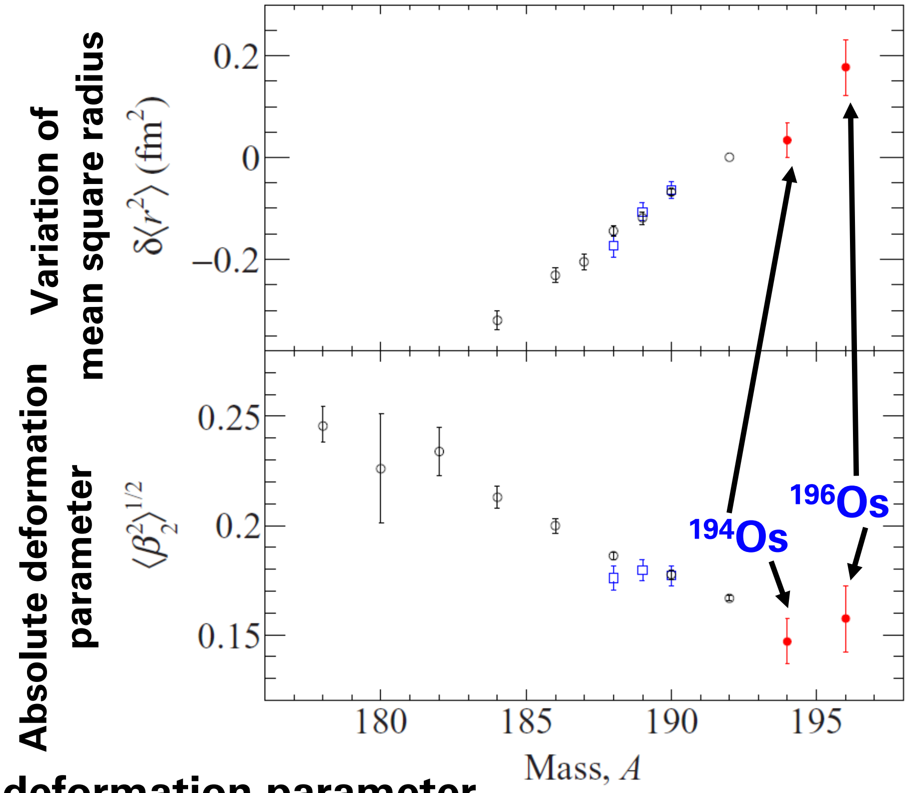

Values of deformation parameter

TABLE II. The quadrupole deformation parameter $\langle \beta_2^2 \rangle^{1/2}$ values for $^{194,196}Os$ from this work and theoretical models [8,53,54,56].

A	This work	HF	SCCM	TRS	FRDM
194	0.147(10)	0.14	0.14	0.16	0.153
196	0.157(15)		0.11	0.12	0.119

exp. — theory

Oblate deformation
Tri-axial asymmetry

H. Choi et al., Phys. Rev. C 102, 034309 (2020).

Spectroscopy of neutron-rich actinide nuclei

r-process nucleosynthesis

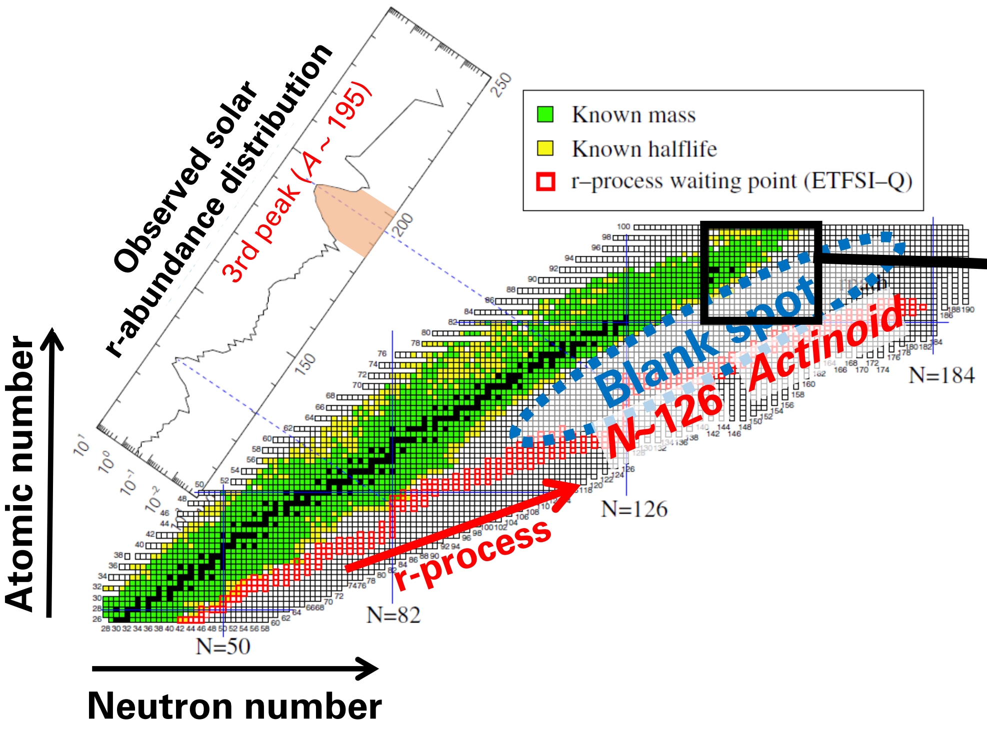

H. Grawe et al., Rept. Prog. Phys. 70, 1525 – 1582 (2007).

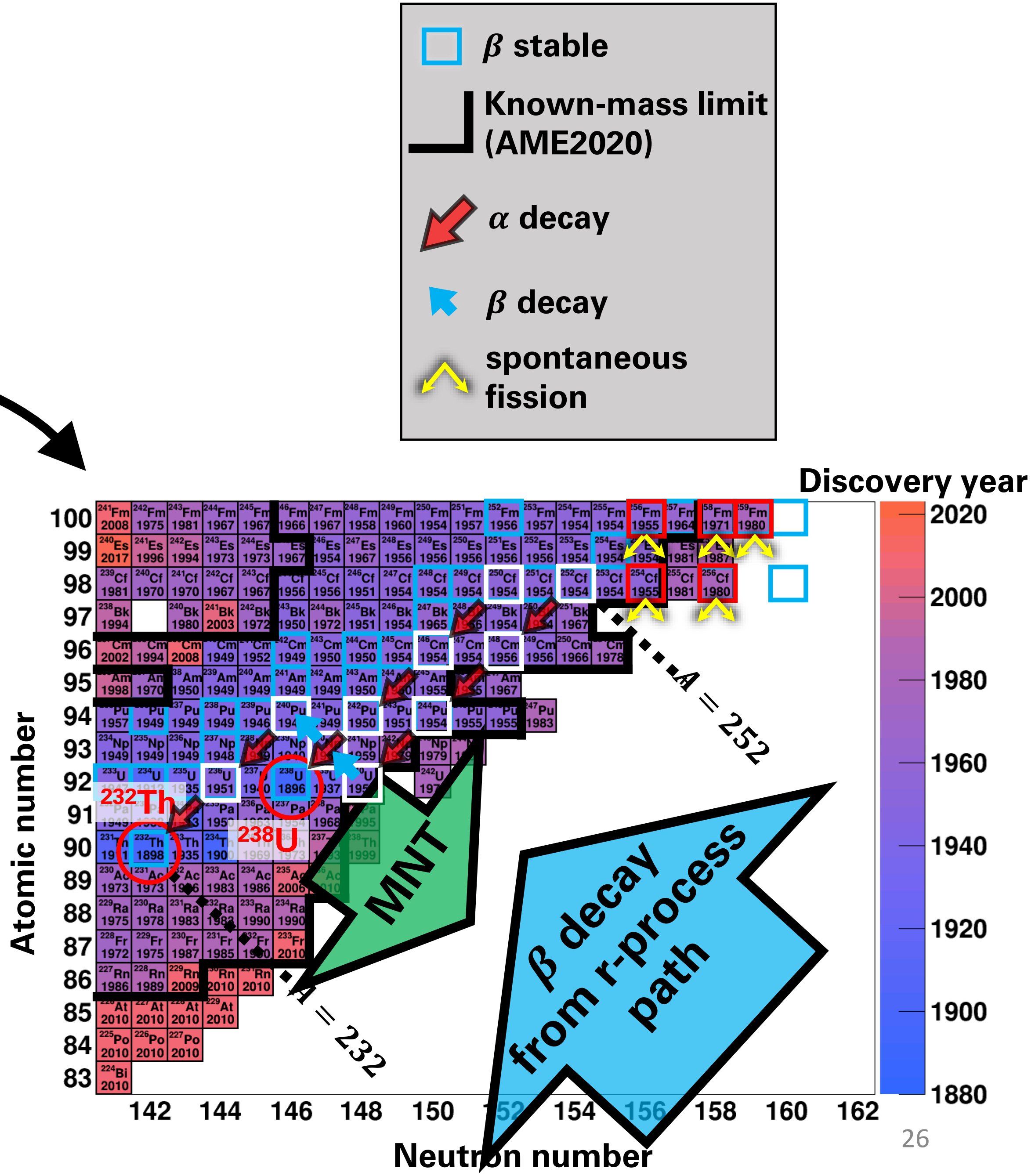

- **Decay spectroscopy**
  - Half life
  - Decay scheme
- **Laser spectroscopy**
  - Charge radius
  - Magnetic dipole moment
  - Electric quadrupole moment
- **Mass spectroscopy**

Nuclear deformation

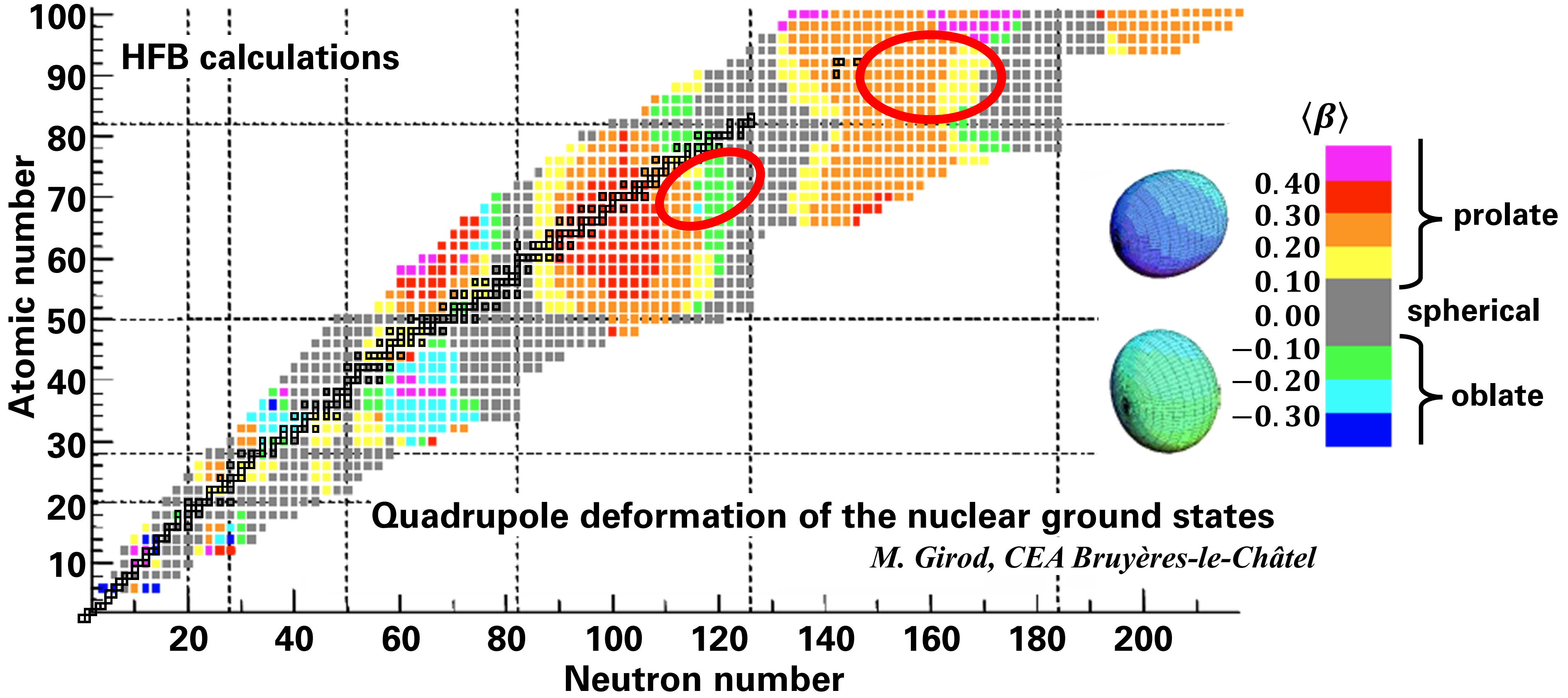

- The shape is one of the most fundamental properties of an atomic nucleus.
  Interplay of macroscopic properties of the nuclear matter and microscopic shell effects
- In some areas of the nuclear chart, the shape is very sensitive to structural effects and can change from one nucleus to its neighbor.
- Excitation energy, Angular momentum
  →Rearrangement of the orbital configuration, Dynamic response to nuclear rotation
  →Shape change
- Mixing of wave functions → Shape coexistence

Single-particle levels around actinoid elements

Proton

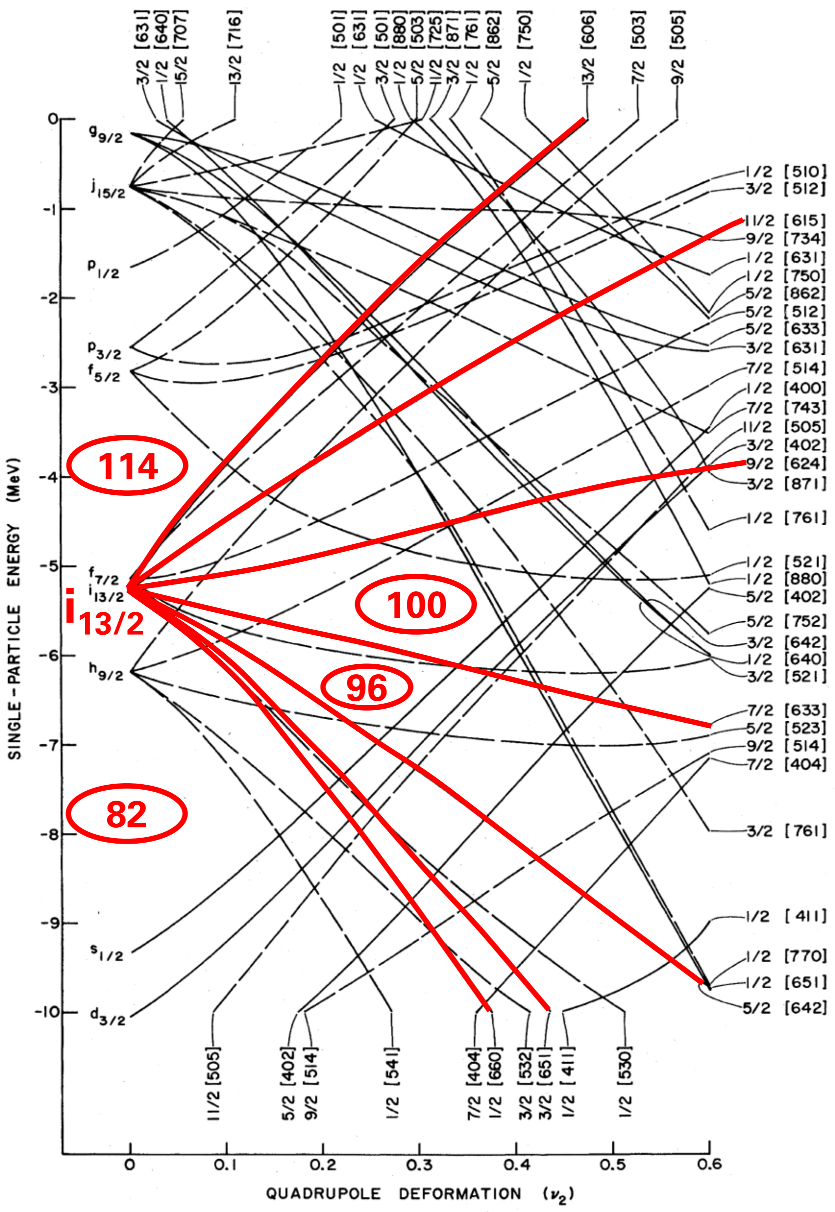

Neutron

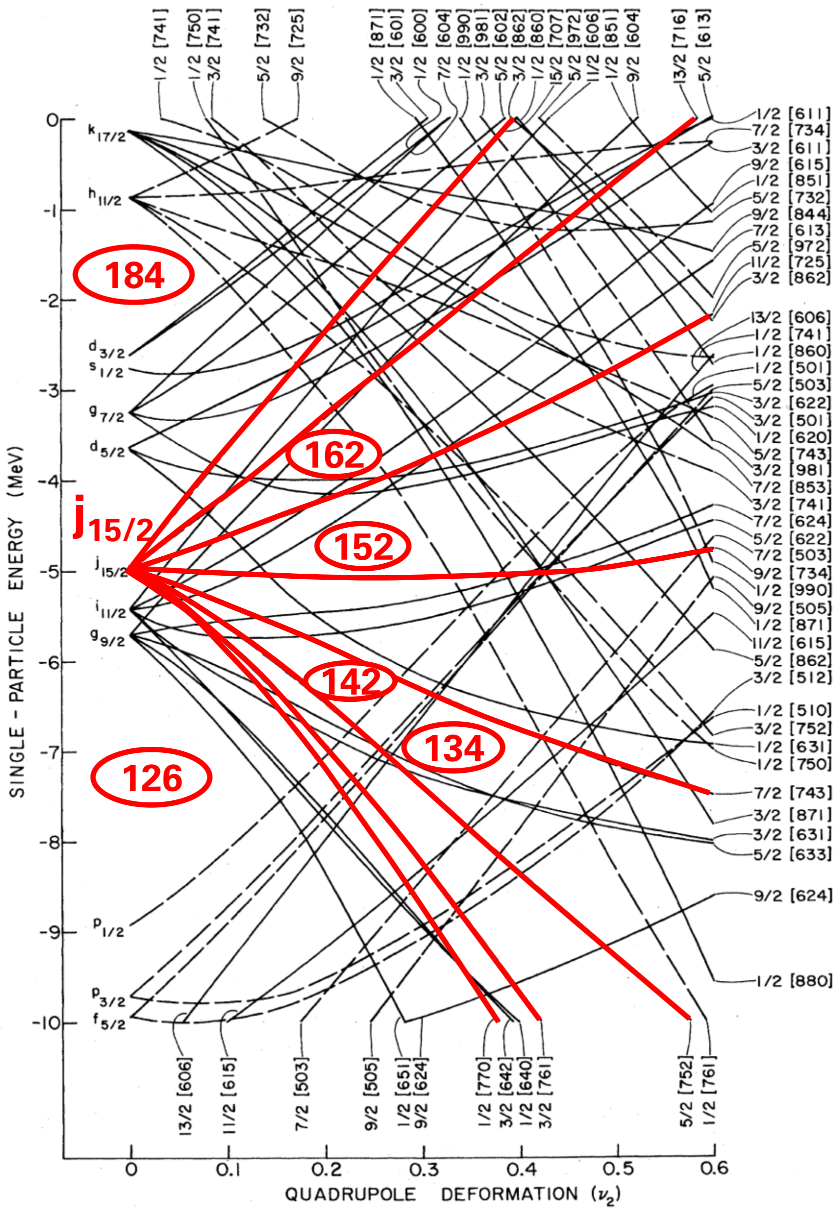

R.R. Chasman et al., Rev. Mod. Phys. 49, 833 (1977).

Evolution of single-particle energies

***N* = 155 isotone**

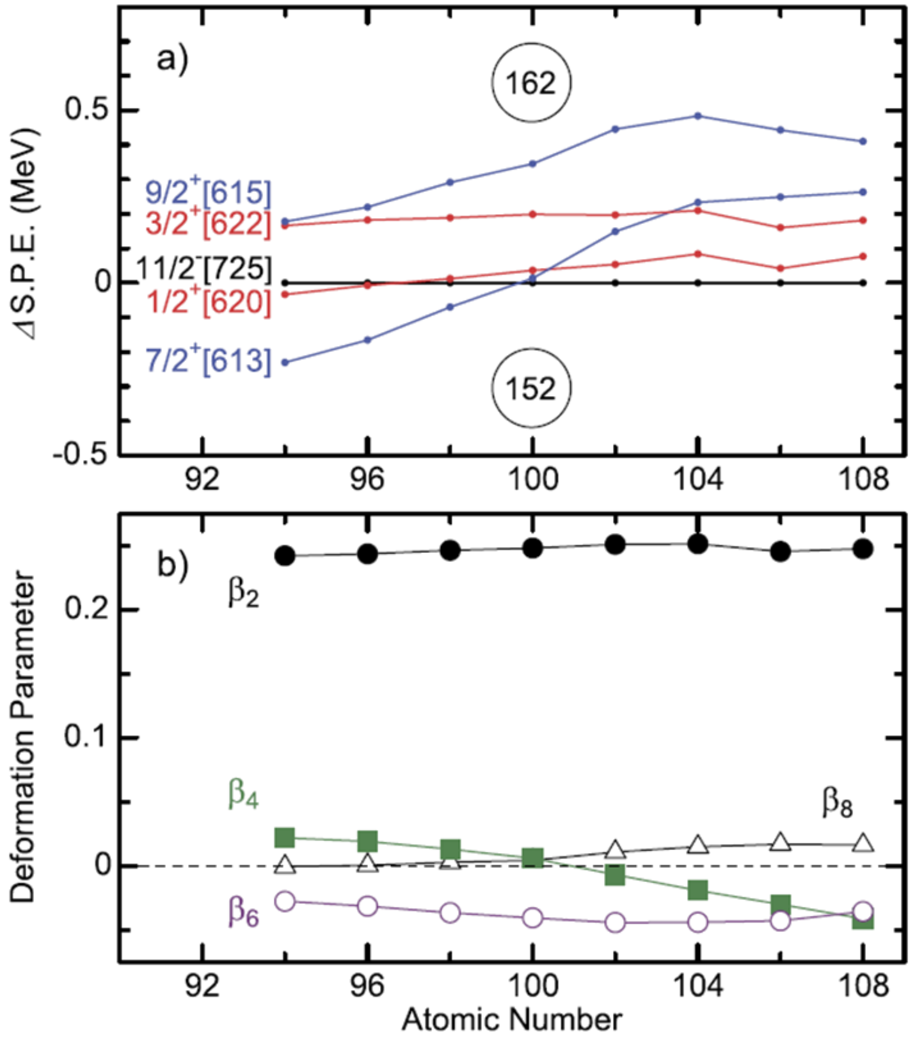

Pairing correlation (p-n, n-n, p-p residual interactions) makes the single-particle energies varied, even their ordering.

- Deformation
- Fission

The studies of the nuclear structure with the measurements of spin-parity, electromagnetic moment of the ground and excited states by β-γ spectroscopy and laser spectroscopy are important to investigate those nuclear properties.

M. Asai et al., Nucl. Phys. A 944, 308 (2015).

Evolution of nuclear shapes

DFT calculations

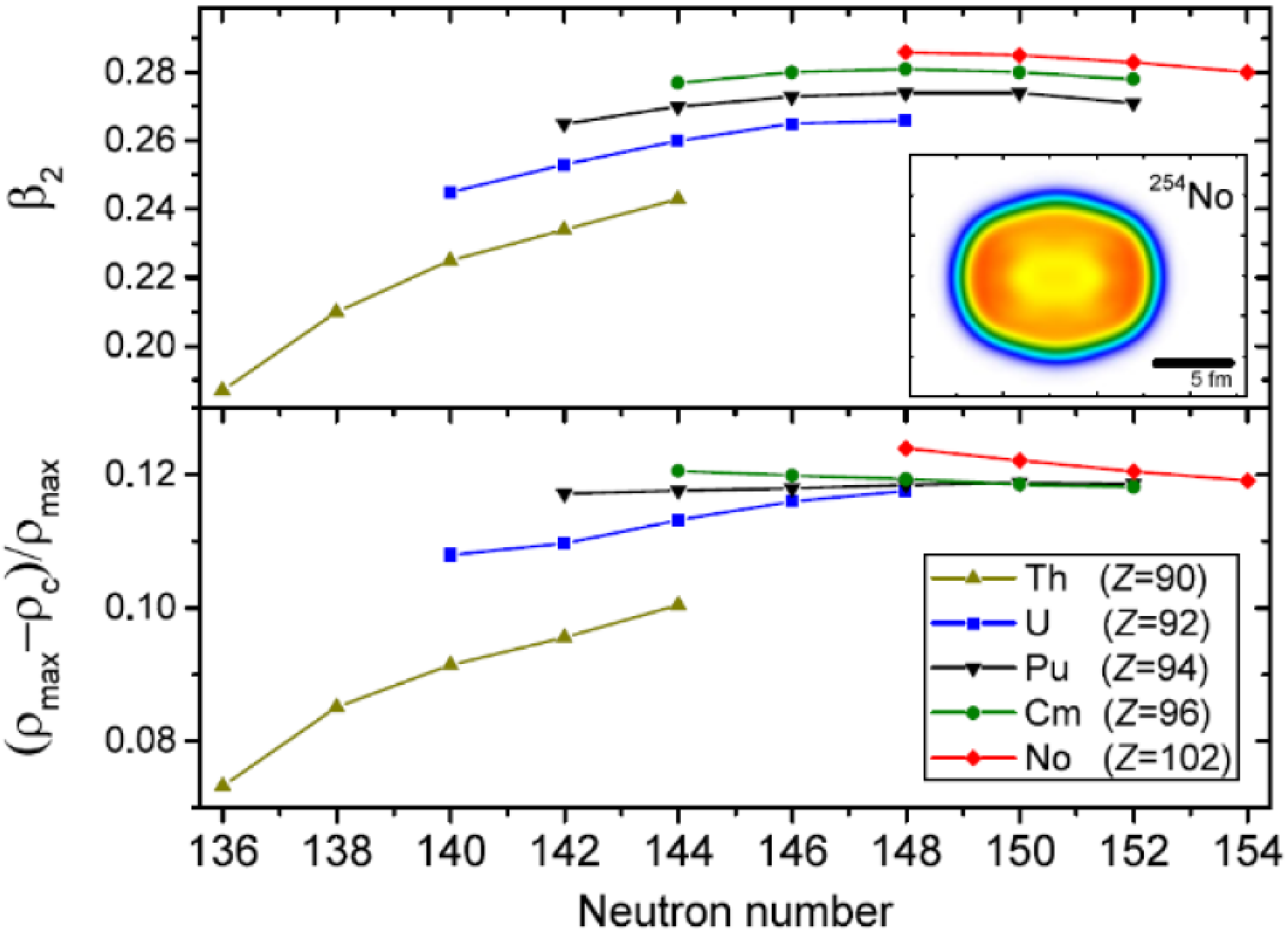

S. Raeder et al., Phys. Rev. Lett 120, 232503 (2018).

Mass spectroscopy of neutron-rich actinoids

^{238}U (10.75 MeV/nucleon) + ^{198}Pt (12.5 mg/cm^2)

TOF spectrum of MRTOF-MS

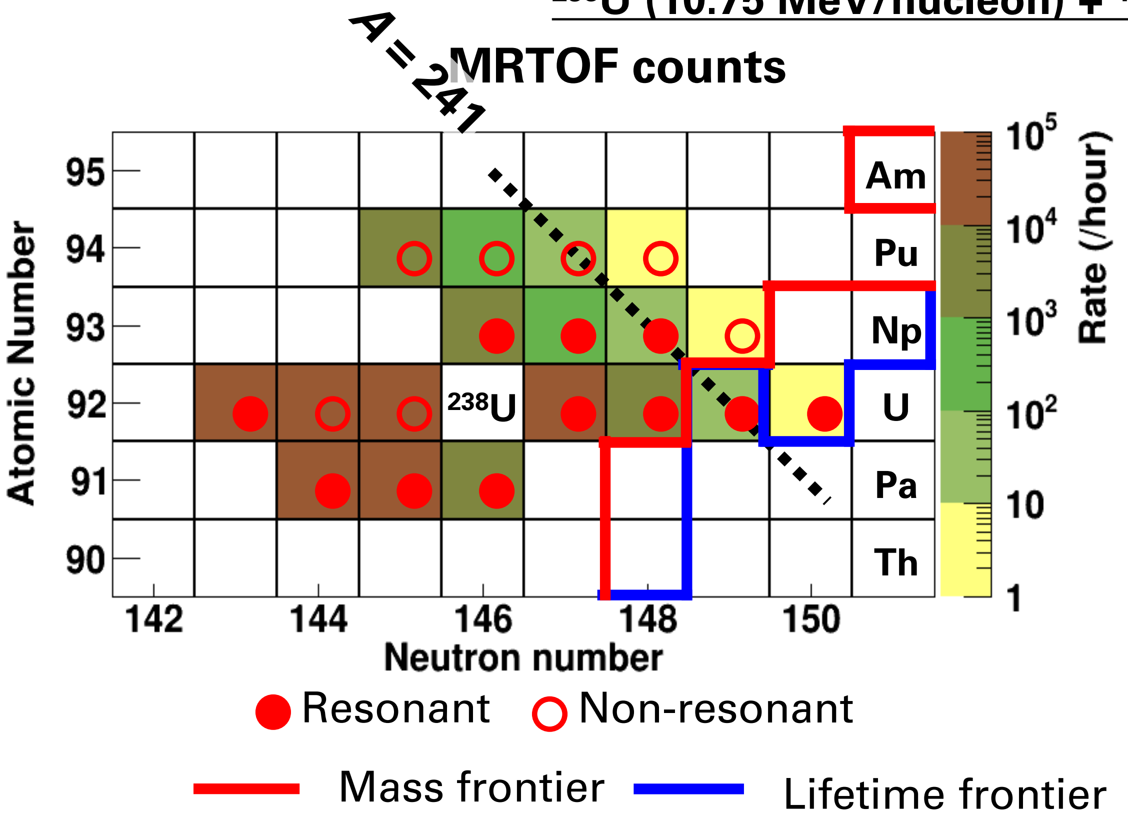

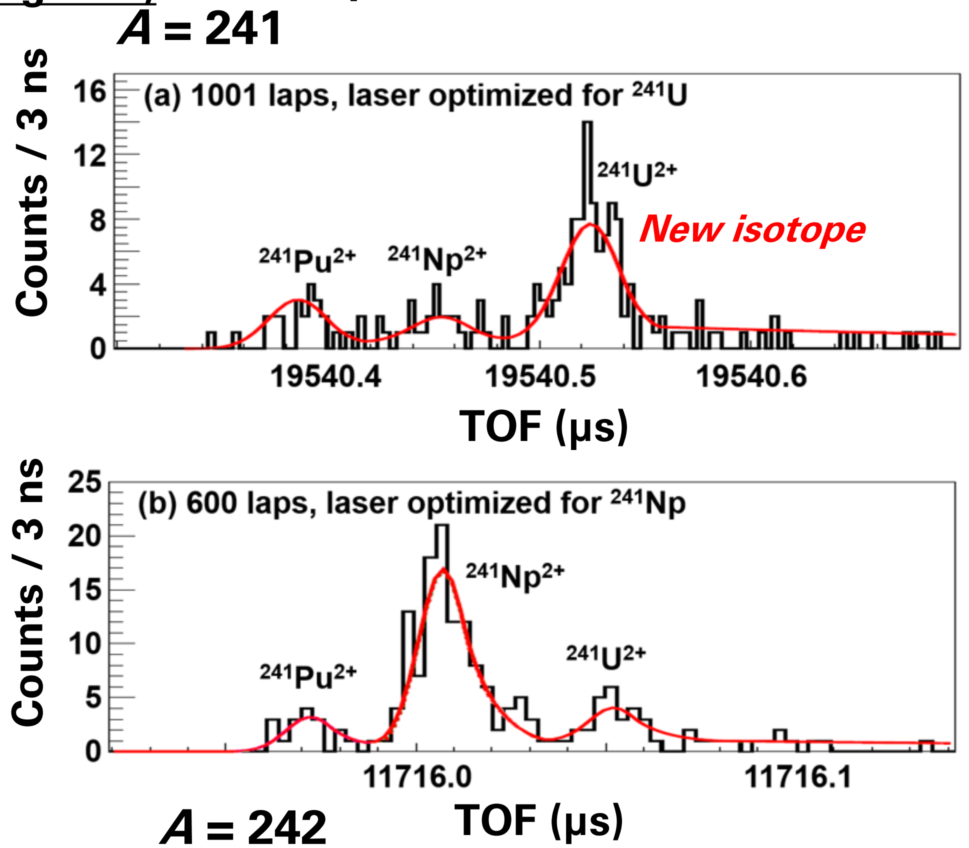

Mass difference from AME2020

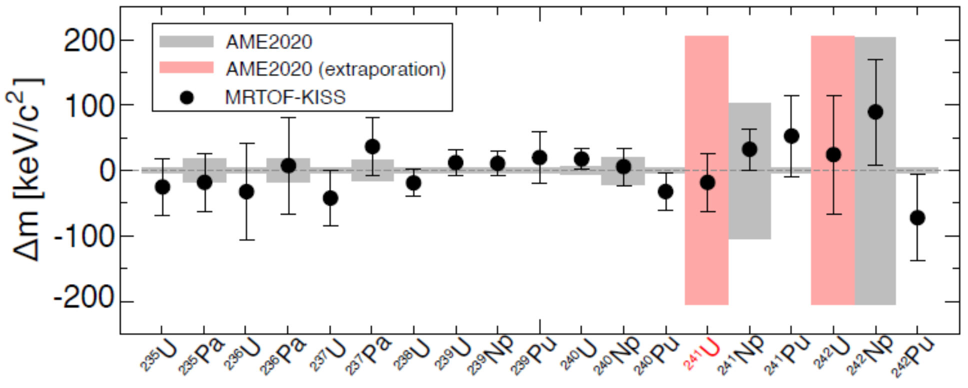

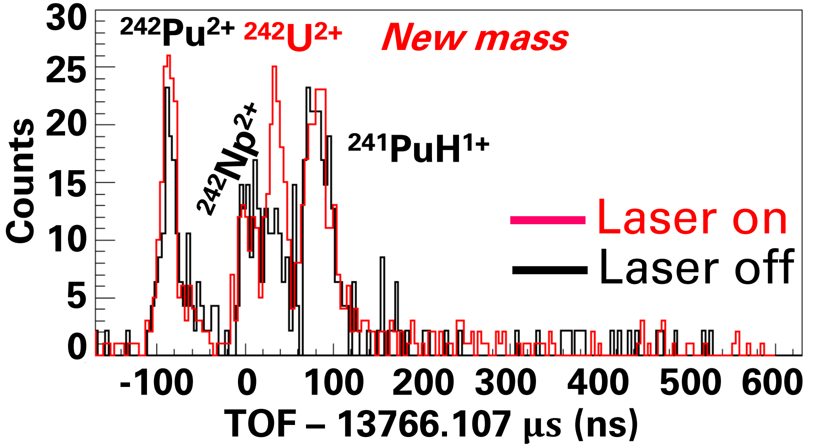

T. Niwase et al., Phys. Rev. Lett. 130, 132502 (2023).

Beyond KISS: KISS-1.5

"Don't separate, but measure multiple species at once"

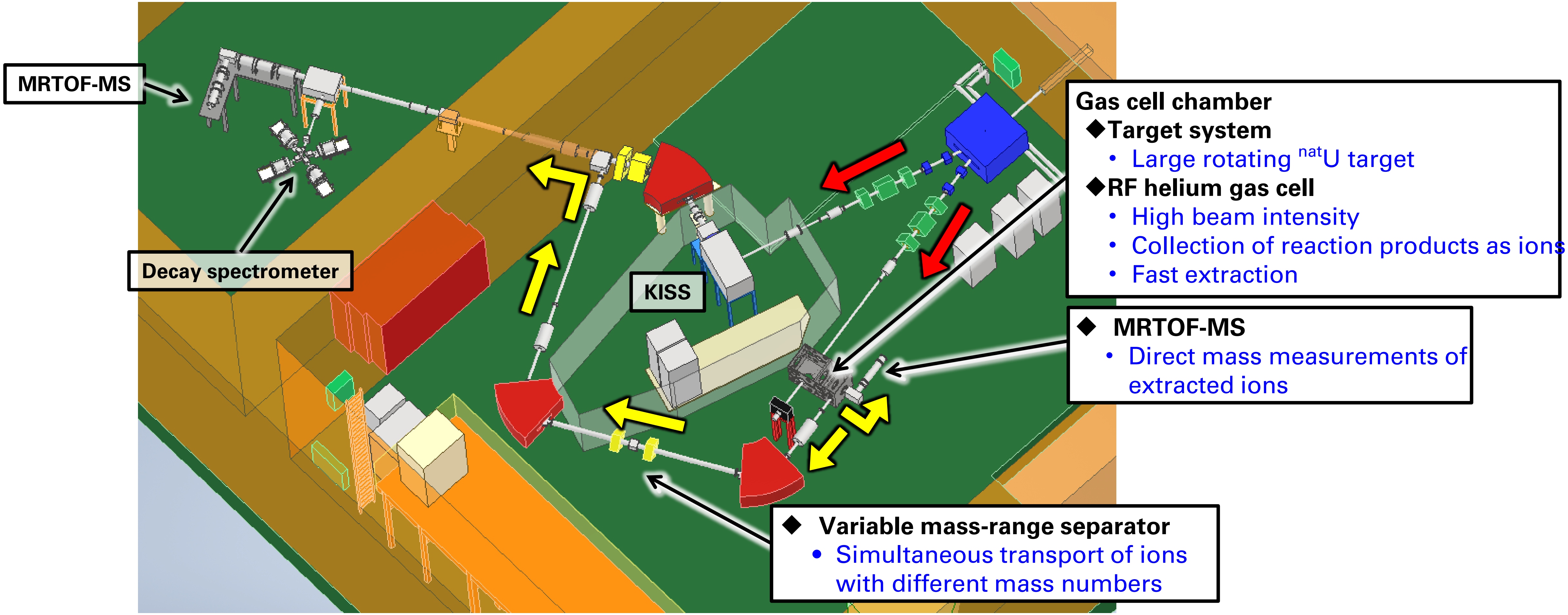

	Primary beam	Total efficiency	Simultaneous measured nuclides	Efficacy
KISS	~ 10 pnA	<0.1%	1	1
KISS-1.5	100 pnA	>1%	> 10	100 ~ 1000
	◆ Target system ◆ RF helium gas cell	◆ RF helium gas cell	◆ RF helium gas cell ◆ MRTOF-MS ◆ Variable mass-range separator	

Expected yields at KISS-1.5

^{238}U (9.4 MeV/nucleon, 100 pnA) + ^{nat}U (13 mg/cm^2)

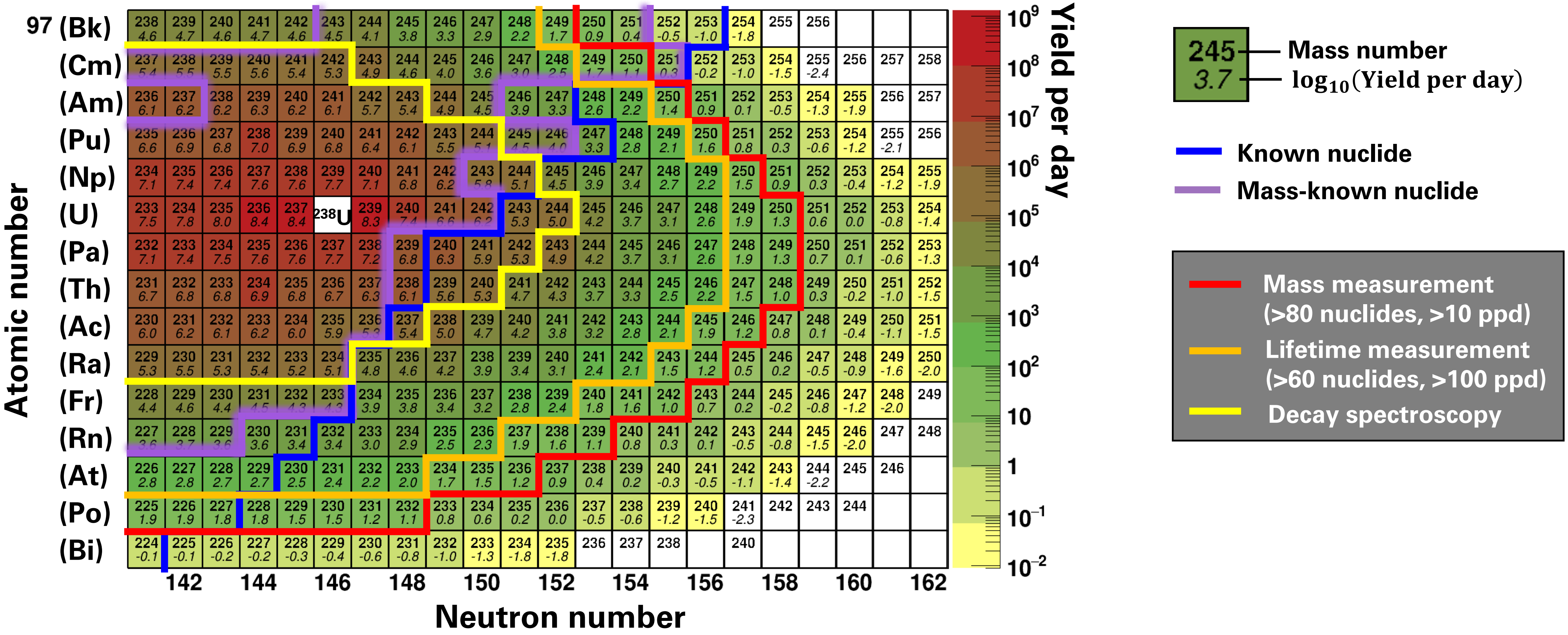

Fission probability of 90% was assumed.
Extraction efficiency of 1% was assumed.

Mass of actinoids and r-process nucleosynthesis

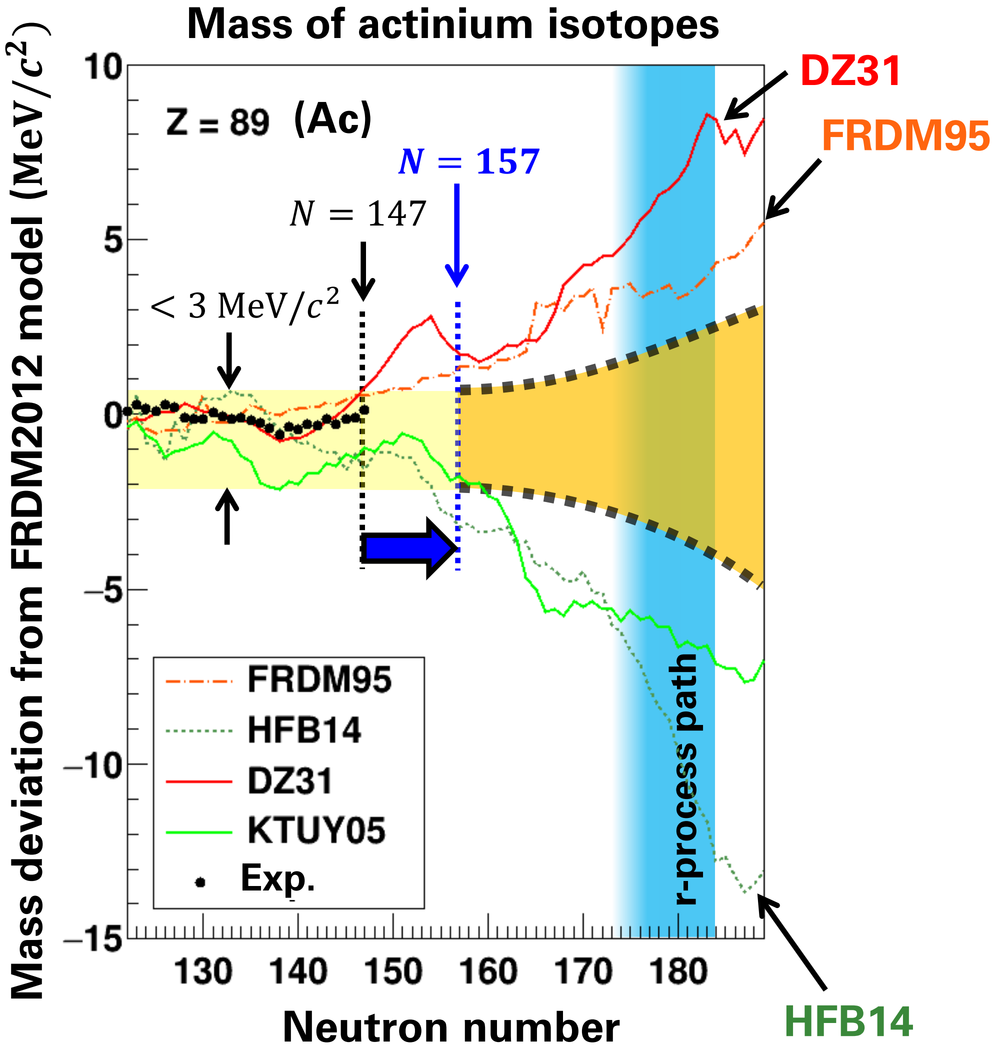

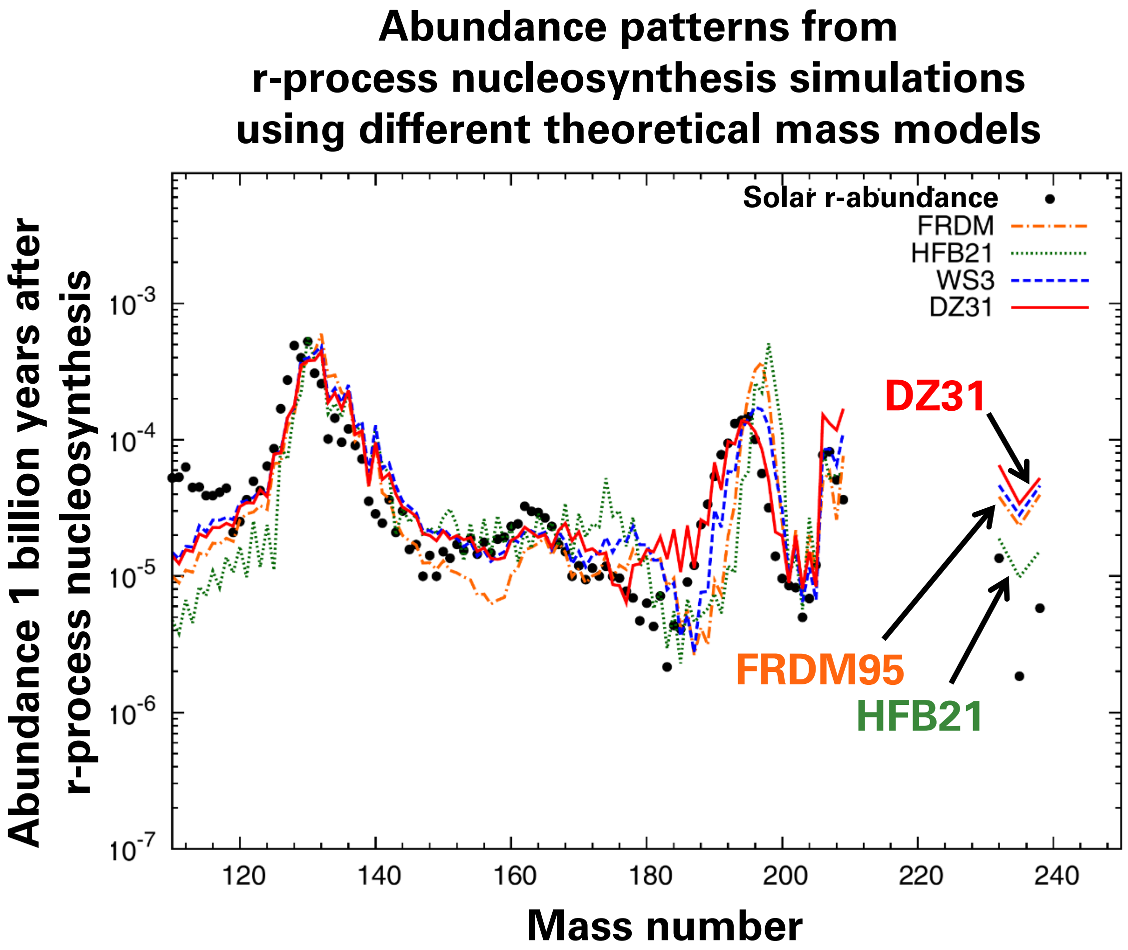

J.J. Mendoza-Temis et al., Phys. Rev. C 92, 055805 (2015).

Obtaining nuclear spectroscopic data for a wide range of neutron-rich actinoid nuclei reduces theoretical uncertainties in evaluating symmetry energies and understanding nuclear structure, allowing for the improvement of more reliable nuclear models.

Comprehensive understanding of r-process nucleosynthesis

- Synthesis process of uranium and thorium
- Fission cycling
- Abundance pattern
- Light curve of kilonova (Spontaneous fission of ^{254}Cf)

Summary

Spectroscopy of nuclei around $N = 126$ and neutron-rich actinides from astrophysical interest.

Evolution of single-particle energies and nuclear shapes.

- **KISS**
  - Nuclear production by MNT reactions
  - Collection by argon gas cell
  - Element selection by laser resonance ionization
  - Mass selection by ISOL

- **Equipments**
  - MSPGC + HPGe detectors: Lifetime measurement, β-γ spectroscopy
  - Excitation laser: Laser spectroscopy
  - MRTOF-MS: Mass spectrometry

- **Beyond KISS: KISS-1.5**
  - Large rotating uranium target
  - RF helium gas cell
  - Variable Mass-Range Separator
  - 100 ~ 1000 times higher efficacy than KISS
  - More than 80 new isotopes with their precise mass measurements